Science Advances
AAAS

advances.sciencemag.org/cgi/content/full/6/23/eaba3471/DC1

Supplementary Materials for

Sequence-based engineering of dynamic functions of micrometer-sized DNA droplets

Yusuke Sato, Tetsuro Sakamoto, Masahiro Takinoue*

*Corresponding author. Email: takinoue@c.titech.ac.jp

Published 3 June 2020, *Sci. Adv.* **6**, eaba3471 (2020)
DOI: 10.1126/sciadv.aba3471

The PDF file includes:

Other Supplementary Material for this manuscript includes the following:

(available at advances.sciencemag.org/cgi/content/full/6/23/eaba3471/DC1)

Oligonucleotide sequences

The sequences of the oligonucleotide strands were designed using the web software NUPACK (*30*). Sequences are shown in tables S1–S3 and S5. To ensure the efficient formation of motifs, flexibility of the stem was introduced by inserting two spacer bases (TT or rUrU) at the center of the junction. Each strand was named N-*i*_*l*_M, where 'N' represents the name of the motif for which the strand is used, '*i*' is a strand identification number, '*l*' is the length of the sticky end (in nucleotides), and 'M' is a modified fluorescent molecule. In the tables, the sticky ends and modified fluorescent molecules are shown in black, the spacer bases in grey, and complementary parts in the stems in the same color.

Table S1. Y-motif sequences

Name	Sequence (5` – 3`)
Y-1_12	GCTAGCGCTAGCCAGTGAGGACGGAAGTTTGTCGTAGCATCGCACC
Y-2_12	GCTAGCGCTAGCCAACCACGCCTGTCCATTACTTCCGTCCTCACTG
Y-3_12	GCTAGCGCTAGCGGTGCGATGCTACGACTTTGGACAGGCGTGGTTG
Y-1_10	GACTCGAGTCCAGTGAGGACGGAAGTTTGTCGTAGCATCGCACC
Y-2_10	GACTCGAGTCCAACCACGCCTGTCCATTACTTCCGTCCTCACTG
Y-3_10	GACTCGAGTCGGTGCGATGCTACGACTTTGGACAGGCGTGGTTG
Y-1_8	GCTCGAGCCAGTGAGGACGGAAGTTTGTCGTAGCATCGCACC
Y-2_8	GCTCGAGCCAACCACGCCTGTCCATTACTTCCGTCCTCACTG
Y-3_8	GCTCGAGCGGTGCGATGCTACGACTTTGGACAGGCGTGGTTG
Y-1_6	GCTAGCCAGTGAGGACGGAAGTTTGTCGTAGCATCGCACC
Y-2_6	GCTAGCCAACCACGCCTGTCCATTACTTCCGTCCTCACTG
Y-3_6	GCTAGCGGTGCGATGCTACGACTTTGGACAGGCGTGGTTG
Y-1_4	GCGCCAGTGAGGACGGAAGTTTGTCGTAGCATCGCACC
Y-2_4	GCGCCAACCACGCCTGTCCATTACTTCCGTCCTCACTG
Y-3_4	GCGCGGTGCGATGCTACGACTTTGGACAGGCGTGGTTG
Y-1_2	GCCAGTGAGGACGGAAGTTTGTCGTAGCATCGCACC
Y-2_2	GCCAACCACGCCTGTCCATTACTTCCGTCCTCACTG
Y-3_2	GCGGTGCGATGCTACGACTTTGGACAGGCGTGGTTG
Y-2_0_FAM	[6-FAM]-CAACCACGCCTGTCCATTACTTCCGTCCTCACTG

Table S2. Sequences of motifs with four and six branches with 8-nucleotide sticky ends

Name	Sequence (5` – 3`)
Four-1_8	GCTCGAGCGCTGGACTAACGGAACGGTTAGTCAGGTATGCCAGCAC
Four-2_8	GCTCGAGCGTGCTGGCATACCTGACTTTCGCAAATTTACAGCGCCG
Four-3_8	GCTCGAGCCGGCGCTGTAAATTTGCGTTCATCACTTGGGACCATGG
Four-4_8	GCTCGAGCCCATGGTCCCAAGTGATGTTCCGTTCCGTTAGTCCAGC
Four-2_0_Cy3	[Cy3]-GTGCTGGCATACCTGACTTTCGCAAATTTACAGCGCCG
Six-1_8	GCTCGAGCGCTGGACTAACGGAACGGTTAGTCAGGTATGCCAGCAC
Six-2_8	GCTCGAGCCTCAGAGAGGTGACAGCATTCCGTTCCGTTAGTCCAGC
Six-3_8	GCTCGAGCCCATGGTCCCAAGTGATGTTTGCTGTCACCTCTCTGAG
Six-4_8	GCTCGAGCCGGCGCTGTAAATTTGCGTTCATCACTTGGGACCATGG
Six-5_8	GCTCGAGCCAGACGTCACTCTCCAACTTCGCAAATTTACAGCGCCG
Six-6_8	GCTCGAGCGTGCTGGCATACCTGACTTTGTTGGAGAGTGACGTCTG
Six-5_0_Cy5	[Cy5]-CAGACGTCACTCTCCAACTTCGCAAATTTACAGCGCCG

Table S3. Orthogonal Y-motif (^{orth}Y-motif) sequences

Name	Sequence (5` – 3`)
^{orth}Y-1_8	**CTCGCGAG**AAAGGAACTCTCCGCGTTGACAAAGCCGACACGT
^{orth}Y-2 _8	**CTCGCGAG**GCCTCTGTGTCGCATCTTCGCGGAGAGTTCCTTT
^{orth}Y-3 _8	**CTCGCGAG**ACGTGTCGGCTTTGTCTTGATGCGACACAGAGGC
^{orth}Y-2 _0 _Alexa405	[Alexa405]-GCCTCTGTGTCGCATCTTCGCGGAGAGTTCCTTT

Table S4. T_m and enthalpy changes (ΔH) of the sequences for the Y- and ^{orth}Y-motifs. These parameters were obtained using DINAMelt (*31*) with 350 mM Na^+ and 5 µM DNA (for the stems) and 15 µM DNA (for the sticky ends) in the mode of 'Two State melting (hybridization)' ΔH was calculated based on the nearest-neighbor method.

Sequence pair	T_m [°C]	$-\Delta H$ [kcal/mol]
CAGTGAGGACGGAAGT vs ACTTCCGTCCTCACTG	63.5	122.3
GTCGTAGCATCGCACC vs GGTGCGATGCTACGAC	66.1	129.4
CAACCACGCCTGTCCA vs TGGACAGGCGTGGTTG	67.1	129.6
AAAGGAACTCTCCGCG vs CGCGGAGAGTTCCTTT	64.8	124.7
GACAAAGCCGACACGT vs ACGTGTCGGCTTTGTC	65.7	127.2
GCCTCTGTGTCGCATC vs GATGCGACACAGAGGC	66.0	127.7
GCTCGAGC vs GCTCGAGC	45.9	62.0
CTCGCGAG vs **CTCGCGAG**	45.5	62.8

Table S5. Sequences of six-junction motifs (S-motif) and the chimerized-S-motif (CS-motif)

Name	Sequence
S-1_8	**CTCGCGAG**GCTGGACTAACGGAACGGTTAGTCAGGTATGCCAGCAC
S-2_8	**CTCGCGAG**CTCAGAGAGGTGACAGCATTCCGTTCCGTTAGTCCAGC
S-3_8	**CTCGCGAG**CCATGGTCCCAAGTGATGTTTGCTGTCACCTCTCTGAG
S-4_8	GCTCGAGCCGGCGCTGTAAATTTGCGTTCATCACTTGGGACCATGG
S-5_8	GCTCGAGCCAGACGTCACTCTCCAACTTCGCAAATTTACAGCGCCG
S-6_8	GCTCGAGCGTGCTGGCATACCTGACTTTGTTGGAGAGTGACGTCTG
S-2_0_Cy3	[Cy3]-CTCAGAGAGGTGACAGCATTCCGTTCCGTTAGTCCAGC
S-5_0_Cy5	[Cy5]-CAGACGTCACTCTCCAACTTCGCAAATTTACAGCGCCG
CS-1_8[#]	**CTCGCGAG**GCTGGACTAACGGArArCrGrGrUrUrArGrUrCAGGTATGCCAGCAC
CS-4_8[#]	GCTCGAGCCGGCGCTGTAAATTrUrGrCrGrUrUrCrArUrCACTTGGGACCATGG

[#]The letter "r" precedes a ribonucleotide.

Material compositions

Table S6: Strand concentration to confirm orthogonality

DNA strand name	Final concentration
Y-1_8	5.0 µM
Y-2_8	4.5 µM
Y-3_8	5.0 µM
Y-2_0_FAM	0.5 µM
^{orth}Y-1_8	5.0 µM
^{orth}Y-2_8	4.5 µM
^{orth}Y-3_8	5.0 µM
^{orth}Y-2_0_Alexa405	0.5 µM

Table S7: Strand concentration for the elimination of orthogonality

DNA strand name	Final concentration
Y-1_8	5.000 µM
Y-2_8	4.500 µM
Y-3_8	5.000 µM
Y-2_0_FAM	0.500 µM
^{orth}Y-1_8	5.000 µM
^{orth}Y-2_8	4.500 µM
^{orth}Y-3_8	5.000 µM
^{orth}Y-2_0_Alexa405	0.500 µM
S-1_8	1.650 µM
S-2_8	1.650 µM
S-3_8	1.650 µM
S-4_8	1.650 µM
S-5_8	1.485 µM
S-6_8	1.650 µM
S-5_0_Cy5	0.165 µM

Table S8: Strand concentrations for droplet fission

DNA strand name	Final concentration
Y-1_8	5.000 µM
Y-2_8	4.500 µM
Y-3_8	5.000 µM
Y-2_0_FAM	0.500 µM
^{orth}Y-1_8	5.000 µM
^{orth}Y -2_8	4.500 µM
^{orth}Y-3_8	5.000 µM
^{orth}Y-2_0_Alexa405	0.500 µM
CS-1_8	1.650 µM
S-2_8	1.485 µM
S-3_8	1.650 µM
CS-4_8	1.650 µM
S-5_8	1.485 µM
S-6_8	1.650 µM
S-2_0_Cy3	0.165 µM
S-5_0_Cy5	0.165 µM

Table S9: Strand concentrations for the Janus-shaped DNA droplets

DNA strand name	Final concentration
Y-1_8	5.000 µM
Y-2_8	4.500 µM
Y-3_8	5.000 µM
Y-2_0_FAM	0.500 µM
^{orth}Y-1_8	5.000 µM
^{orth}Y -2_8	4.500 µM
^{orth}Y-3_8	5.000 µM
^{orth}Y-2_0_Alexa405	0.500 µM
CS-1_8	0.165 µM
S-1_8	1.485 µM
S-2_8	1.485 µM
S-3_8	1.650 µM
CS-4_8	0.165 µM
S-4_8	1.485 µM
S-5_8	1.485 µM
S-6_8	1.650 µM
S-2_0_Cy3	0.165 µM
S-5_0_Cy5	0.165 µM

Table S10: Strand concentration for the patchy-like pattern in the DNA droplets

DNA strand name	Final concentration
Y-1_8	5.000 µM
Y-2_8	4.500 µM
Y-3_8	5.000 µM
Y-2_0_FAM	0.500 µM
^{orth}Y-1_8	5.000 µM
^{orth}Y -2_8	4.500 µM
^{orth}Y-3_8	5.000 µM
^{orth}Y-2_0_Alexa405	0.500 µM
CS-1_8	0.825 µM
S-1_8	0.825 µM
S-2_8	1.485 µM
S-3_8	1.650 µM
CS-4_8	0.825 µM
S-4_8	0.825 µM
S-5_8	1.485 µM
S-6_8	1.650 µM
S-2_0_Cy3	0.165 µM
S-5_0_Cy5	0.165 µM

Supplementary Discussion

The state diagram (Fig. 3A in the main text) shows the state-change temperature between the dispersed and droplet-like states (T_d), and between the droplet-like and gel states (T_g). T_d values were 46.3, 48.3, 63.7, 61.3, and 70.3 °C, and T_g values were 12.3, 18.7, 35.7, 41.3, and 53.3 °C, respectively, when the sticky ends (SEs) were 4–12 nt long. The T_d for each SE was higher than the T_m of the SEs. T_g for the Y-motif with a 4-nt SE was also higher than the T_m of the 4-nt SE (Fig. 3B in the main text). Here, we discuss what determines the T_d and T_g in this study.

First, we discuss the T_g. As mentioned in the main text, T_g can be attributed to the stability of SEs and entanglement of motifs. Stable hybridization of SEs results in the formation of static networks of the branched motifs, and the stability is generally characterized by T_m, which depends on the concentration of the DNA. Hence, we experimentally estimated the concentration of the DNA nanostructures in the gel state (Figs. S12 and S13). Under the estimated concentration, the T_m of each SE was higher than the T_g (Fig. 3A in the main text), and the stability of the hybridization of SEs would be enough to form static networks (Fig. S14). The increase in T_g with the number of branches in the motif (Fig. 3C in the main text) could be explained by entanglement of the concentrated motifs. We determined the T_g based on the FRAP experiments, which showed mobility of the motifs. The mobility can be decreased by hybridization of the SEs between the motifs, and an increase in the number of branches in a motif induces structural entanglements that also decrease the mobility of the motifs. The T_g in motifs having four or six branches was higher than their T_m (Fig. 3C in the main text), and the T_g in the six-SE motifs was higher than that with four. Therefore, the effects of the entanglement on T_g would become more dominant than the stability of the hybridization of the SEs.

Next, we discuss the T_d. The T_d values in 4–12-nt SEs were much higher than the T_m of each SE, as described above. The T_m is generally defined as the temperature at which half of the DNA strands in a solution formed double helixes when two complementary DNA strands were present. On the other hand, our motifs have multiple SEs (e.g., Y-motif has three SEs). Thus, the T_m for the SEs should not be considered, but instead, the T_m for the motifs ($T_{m\text{-}Motif}$) at which half of the motifs in a solution are connected should be considered.

In the branched motifs, the hybridization of one of multiple SEs would be sufficient for a connection between the motifs. Based on this idea, we considered that the $T_{m\text{-}Motif}$ can be described as the temperature at which at least one of the multiple SEs can hybridize at a 50 % ratio. It is calculated by the following equation:

$$1 - \big(1 - X(T)\big)^k = 0.5,$$

where $X(T)$ is the hybridization probability of SEs at the temperature T, and k is the number of branches in a motif. The $T_{m\text{-}Motif}$ is calculated by obtaining an $X(T)$ that satisfies this equation.

The $X(T)$ in the motifs with three, four, and six branches (k = 3, 4, and 6) were 21, 16, and 11 %, respectively. This means that the temperature at which the hybridization probability of the SEs for each number of branches exhibit those percentages corresponds to the $T_{m\text{-}Motif}$ (Fig. S15). For example, in the case of a motif having three branches (Y-motif) with a 4-nt SE, 18.8 °C resulted in a 21 % hybridization probability [obtained using NUPACK (*1*)], which represents the $T_{m\text{-}Motif}$ of the Y-motif with 4-nt SEs. Similarly, the $T_{m\text{-}Motif}$ values of the Y-motifs with 6-, 8-, 10-, and 12-nt SEs were 29.2, 53.1, 59.3, and

68.0 °C, respectively (Fig. S16). Those $T_{m\text{-}Motif}$ values were closer to the T_d than was the T_m for the SEs in the bulk solution. Furthermore, the $T_{m\text{-}Motif}$ increased with the number of branches: 53.1 °C for three branches, 55.8 °C for four branches, and 59.6 °C for six branches (Fig. S17). This trend is consistent with the experimental results (Fig. 3C): 63.7, 67.7, and 72.3 °C for three, four, and six branches, respectively. However, there were still gaps between the T_d and $T_{m\text{-}Motif}$, in particular for the shorter SEs, which suggests that another parameter can influence the state-change temperature.

The state diagram also showed that the difference between the T_d and T_g becomes larger with decreasing SE length. As the hybridization stability of the SEs plays a key role in determining the state-change temperature of both the T_d and T_g, the width of the melting range (T_w) provides an indication of the state-change temperature.

In addition to T_m, T_w is also an important parameter for the characterization of melting behavior. T_w can be defined as the difference between the temperatures at the end and the start of DNA melting (Fig. S18). DNA strands transfer from ssDNA to dsDNA states in the range of the T_w and *vice versa*. At the start of the melting, SEs can exhibit weak interactions, and at the end of melting, SEs form stable double helixes. As the self-assembly of motifs into droplets and gel structures results from weak interactions and stable network formations, we speculated that temperature differences between T_d and T_g ($\Delta T_{droplet\text{-}gel}$) were related to T_w.

We calculated T_w for each of the SEs from the melting curve using NUPACK (*1*) (Fig. S19). The $\Delta T_{droplet\text{-}gel}$ and T_w are shown in Fig. S20. $\Delta T_{droplet\text{-}gel}$ and T_w exhibited closer values and the differences between $\Delta T_{droplet\text{-}gel}$ and T_w were smaller for the shorter SEs. Although the entanglement of motifs can influence T_g, as discussed in the main text, this graph suggests that T_w may be one of the parameters that determines the state-change temperature.

Taken together, the entanglements of motifs, multiple SEs in motifs that provide new parameters of $T_{m\text{-}Motif}$, and T_w of SEs could be possible factors influencing the state-change temperature, and their combinatorial effects may determine T_d and T_g. Model-based numerical simulation could be a feasible approach for better understanding what determines T_d and T_g and will be utilized in our future studies.

Supplementary Figs. S1-S30

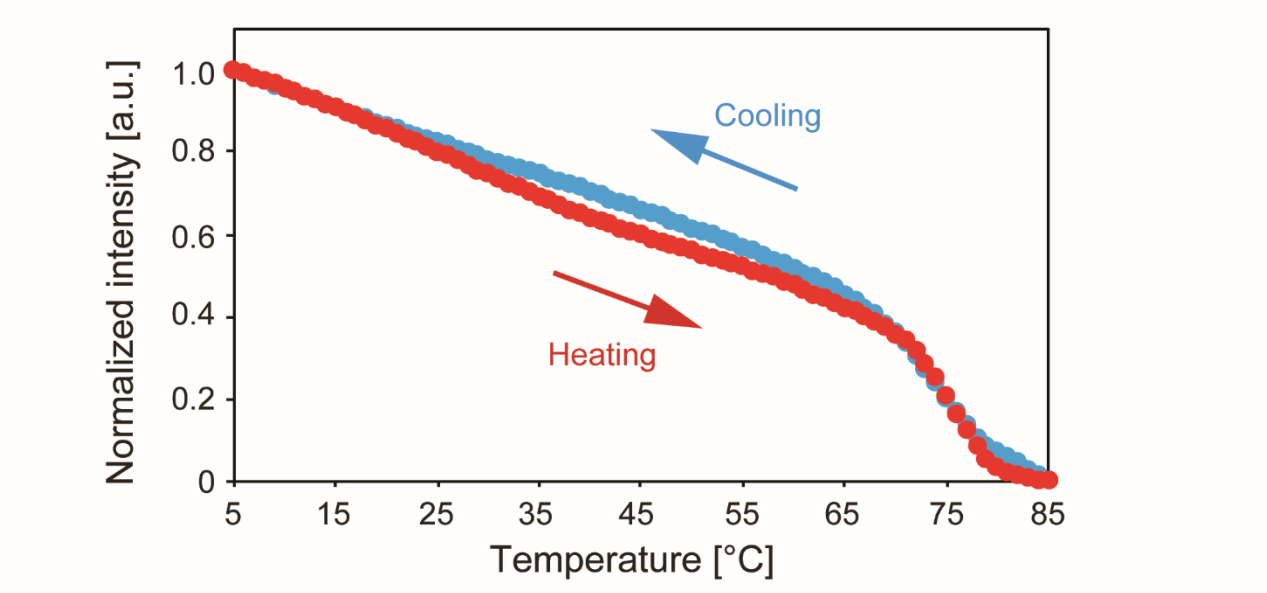

Fig. S1. **Normalized fluorescence intensity during the cooling and heating processes for Y-motifs without sticky ends that cannot connect to one another.** The Y-motifs were formed at 75 °C.

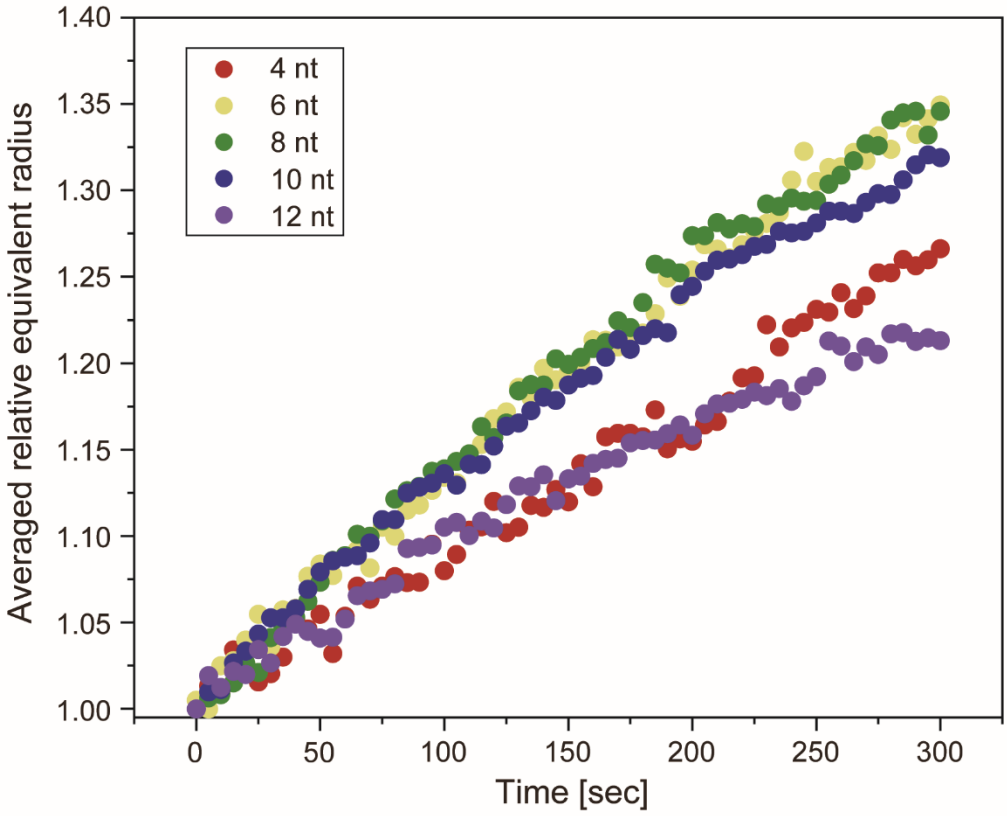

Fig. S2. **Time course of the sizes of DNA droplets composed of Y-motifs at around T_d (the state-change temperature between the dispersed and droplet-like state) of each sticky end (SE).** To measure the averaged relative equivalent radius of the DNA droplets with different nucleotide lengths of SEs, averaged equivalent radius (AER) in each SE was calculated based on the area of the droplets visualized by a confocal microscope. At each time point, the number of droplets counted for the calculation was over 900. The AERs were then divided by the minimum value to obtain the averaged relative equivalent radius.

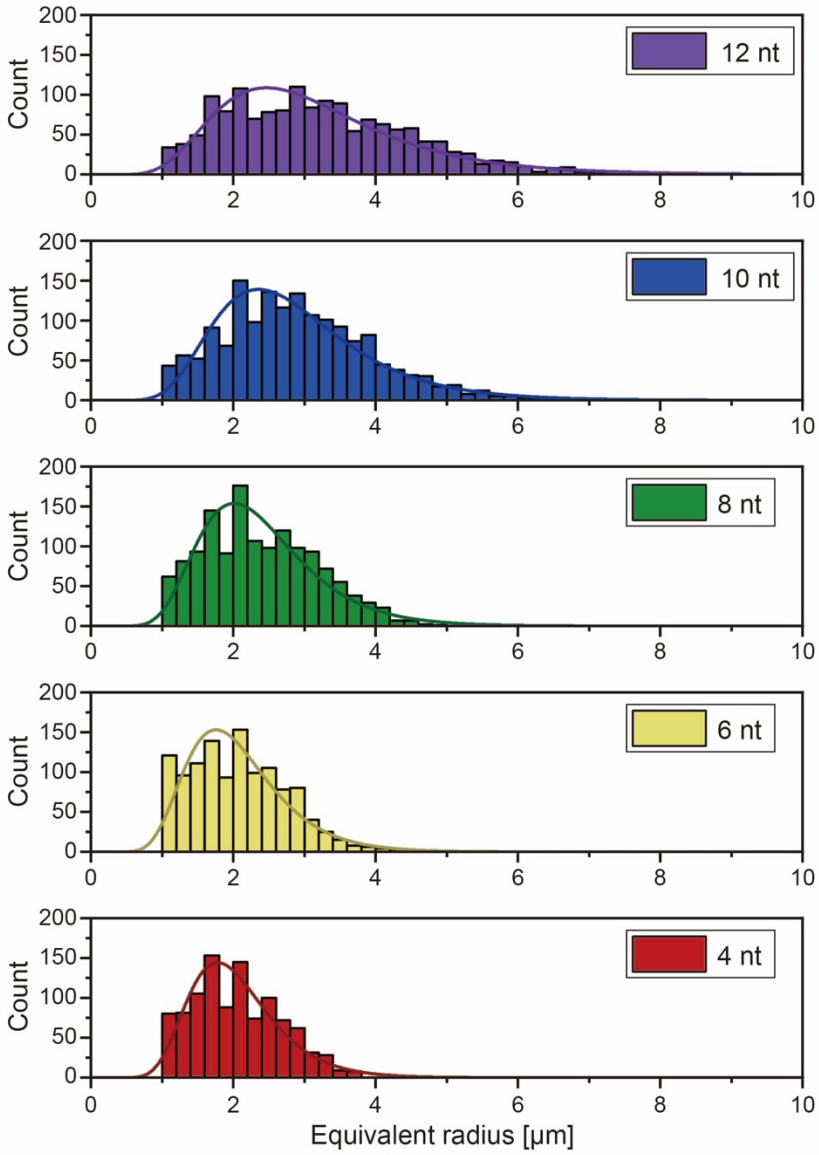

Fig. S3. Particle-**size histograms of the DNA droplets composed of the Y-motifs of each SE.** The data were obtained 700 seconds after the droplet formation. Equivalent radii values were calculated based on the area of the droplets visualized by the confocal microscope. There were over 1,000 droplets for each SE. The colored solid lines in the histogram show fitting curves by a lognormal distribution.

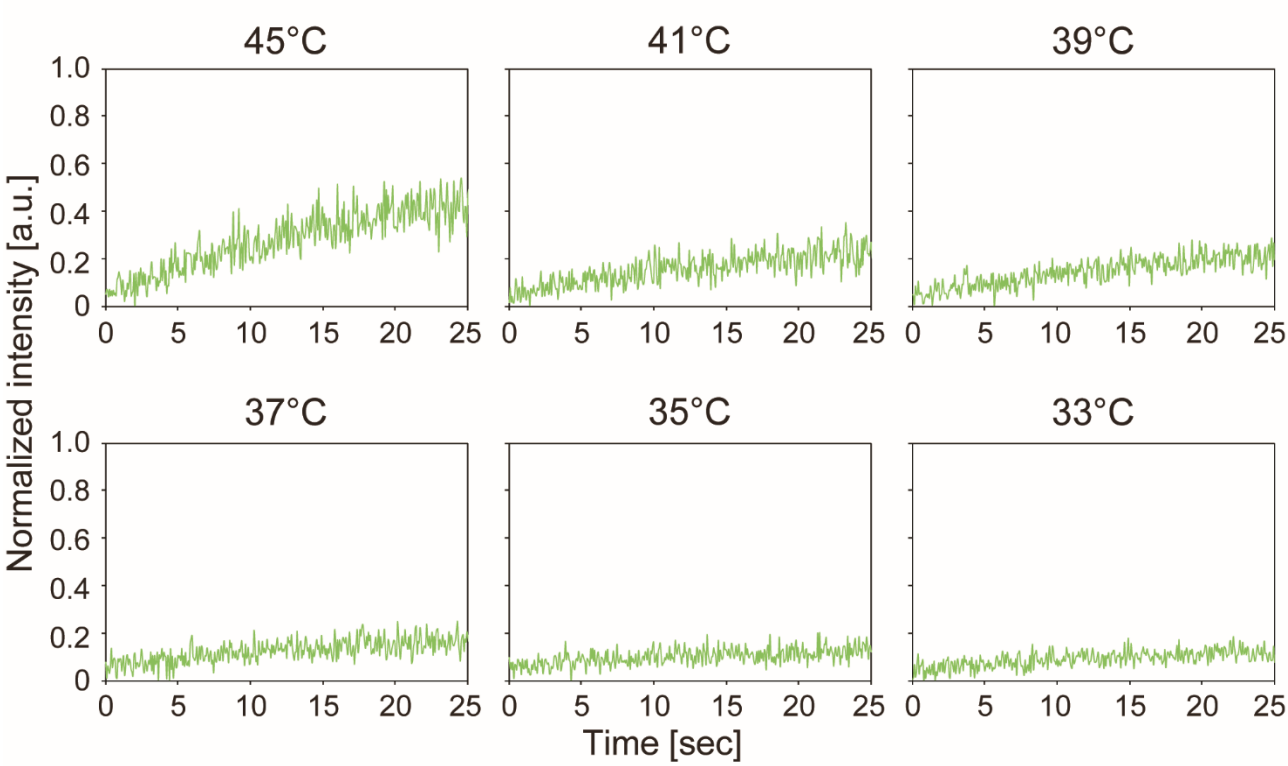

Fig. S4. **Representative results for the FRAP experiments with Y-motifs with 8-nucleotide sticky ends.** The half region of droplets was photo-bleached, and the changes in fluorescence intensity were measured in the bleached regions at each temperature.

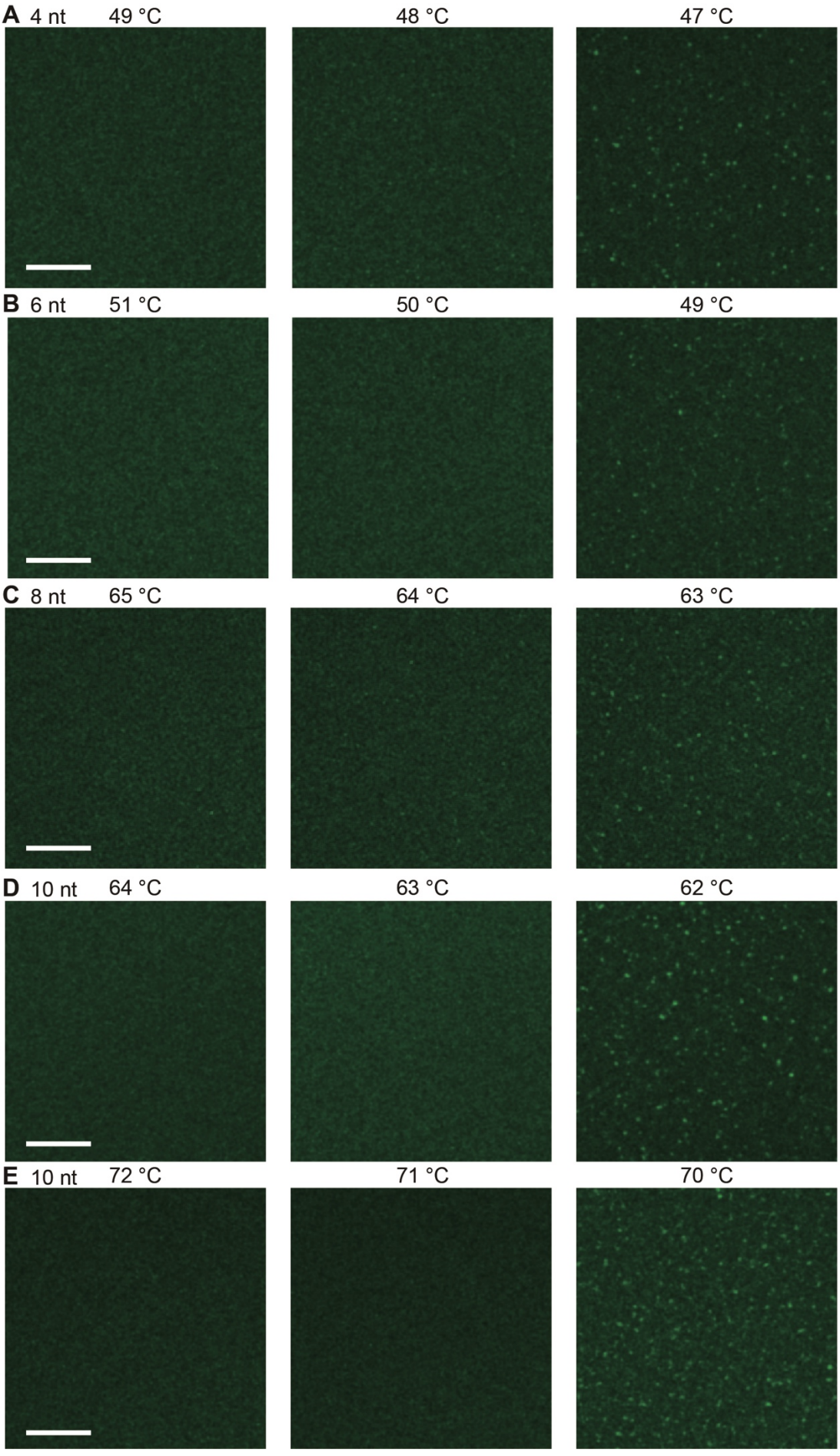
A 4 nt
49 °C
48 °C
47 °C
B 6 nt
51 °C
50 °C
49 °C
C 8 nt
65 °C
64 °C
63 °C
D 10 nt
64 °C
63 °C
62 °C
E 10 nt
72 °C
71 °C
70 °C

Fig. S5. **Microscopy images representing the moment when DNA droplets composed of Y-motifs with 12-, 10-, 8-, 6-, and 4-nucleotide long sticky ends are formed by phase separation in response to decreases in temperature.** Scale bar: 50 μm.

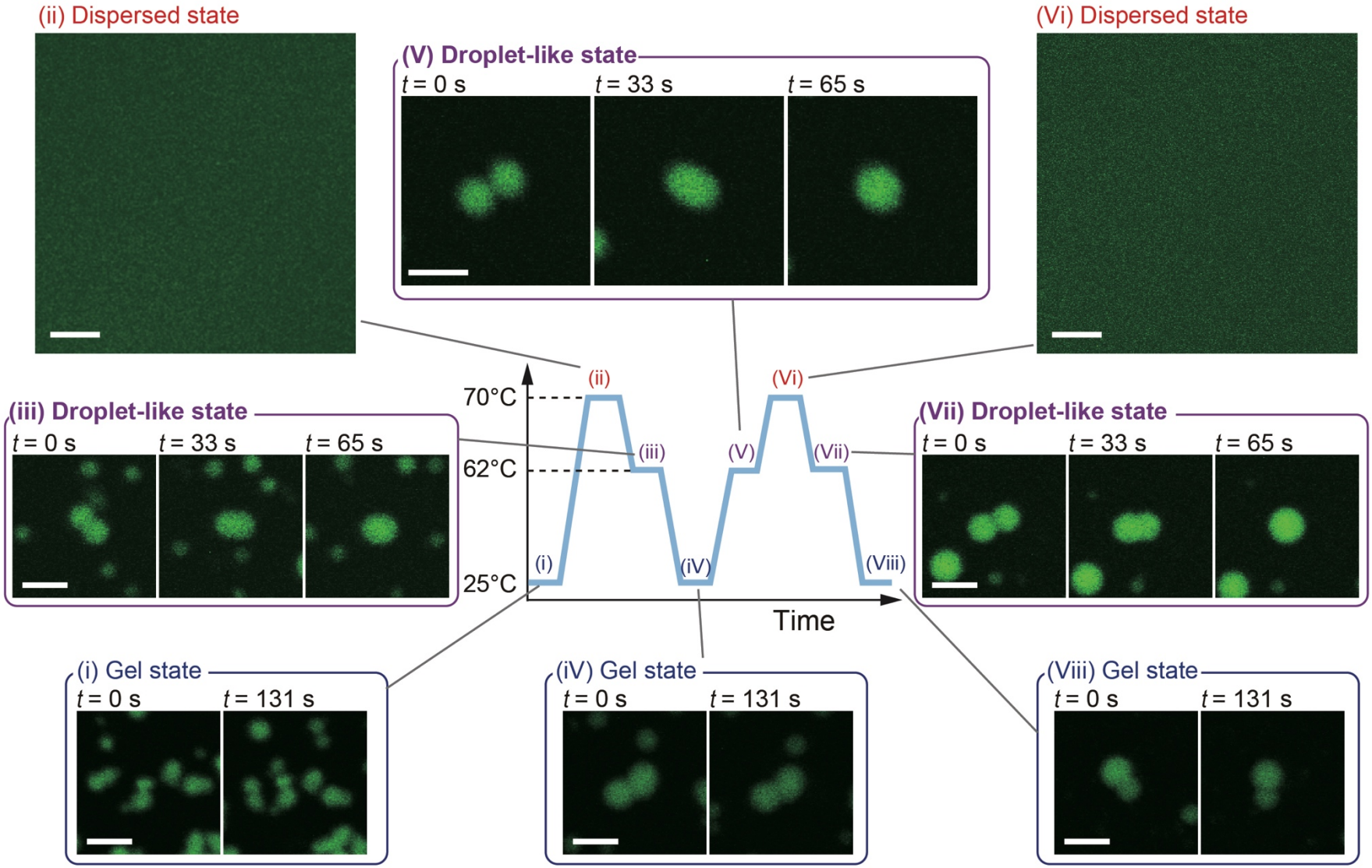

Fig. S6. **Repetitive state changes of Y-motifs with 8-nucleotide sticky ends in response to temperature changes.** The temperature was changed at a rate of ± 20 °C/min. Scale bars: (ii) and (Vi), 30 μm; all others, 10 μm.

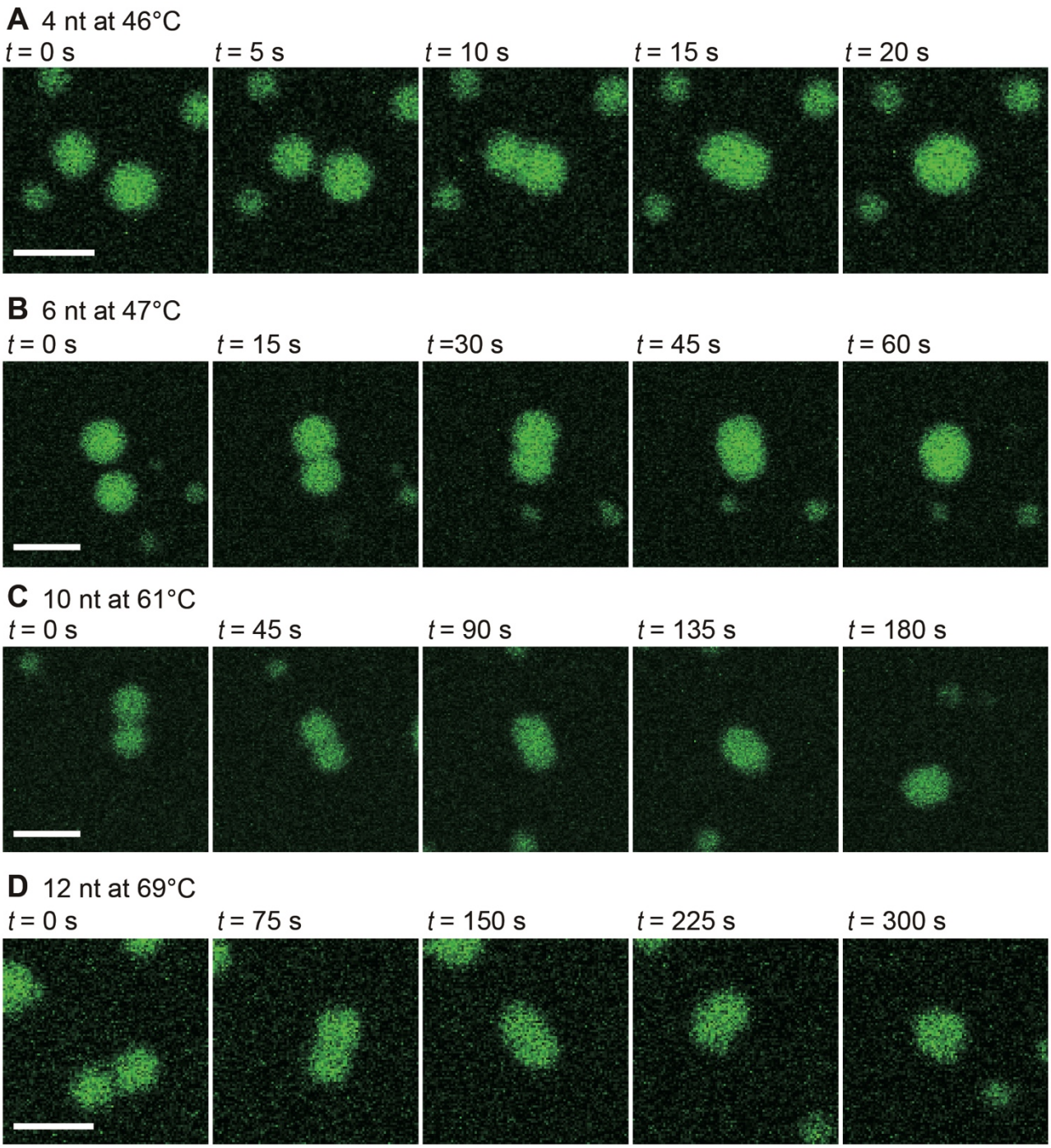

Fig. S7. **Fusion behavior of DNA droplets.** Sequential microscopic images of the droplets composed of Y-motifs that have 4- (**A**), 6- (**B**), 10- (**C**), and 12-nucleotide (**D**) sticky ends. Scale bars: 10 μm.

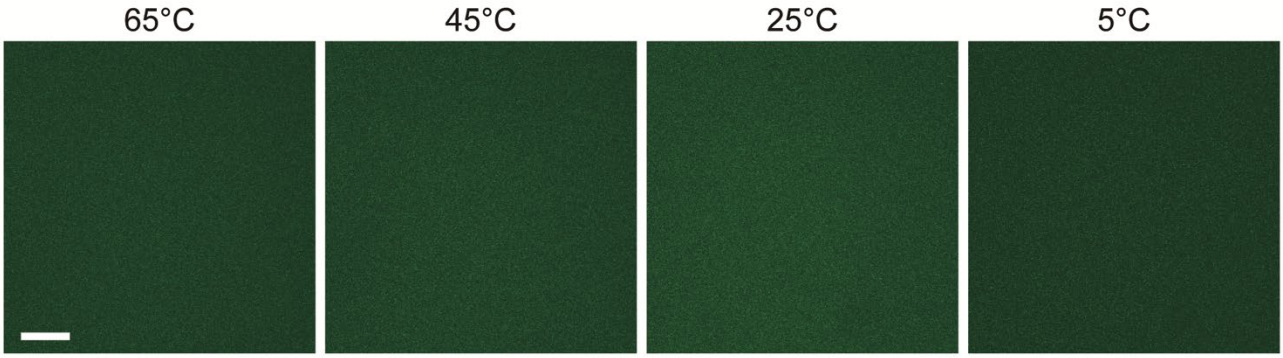

Fig. S8. **Microscopy images for Y-motifs with 2-nucleotide sticky ends visualized at the temperatures shown above the images.** The sample solution in the observation chamber was incubated at 85 °C for 3 min, and then the temperature was decreased to 5 °C at a rate of –1 °C/min. During the annealing process, no micrometer-sized structures were observed. Scale bar: 100 μm.

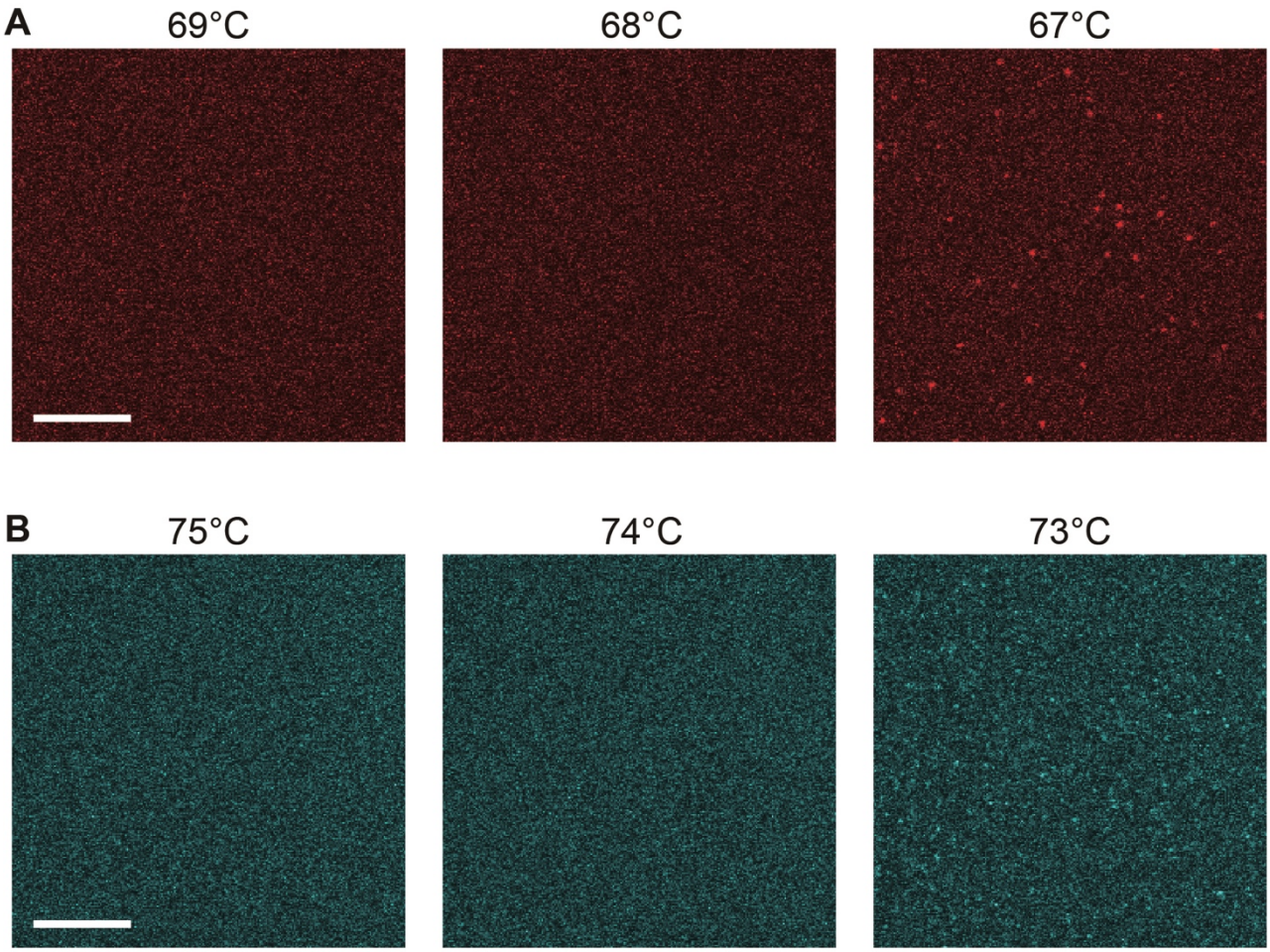

Fig. S9. **Microscopy images representing the moment when DNA droplets composed of motifs having four (A) and six branches with 8-nucleotide sticky ends (B) are formed by phase separation in response to temperature decreases.** Scale bars: 50 μm.

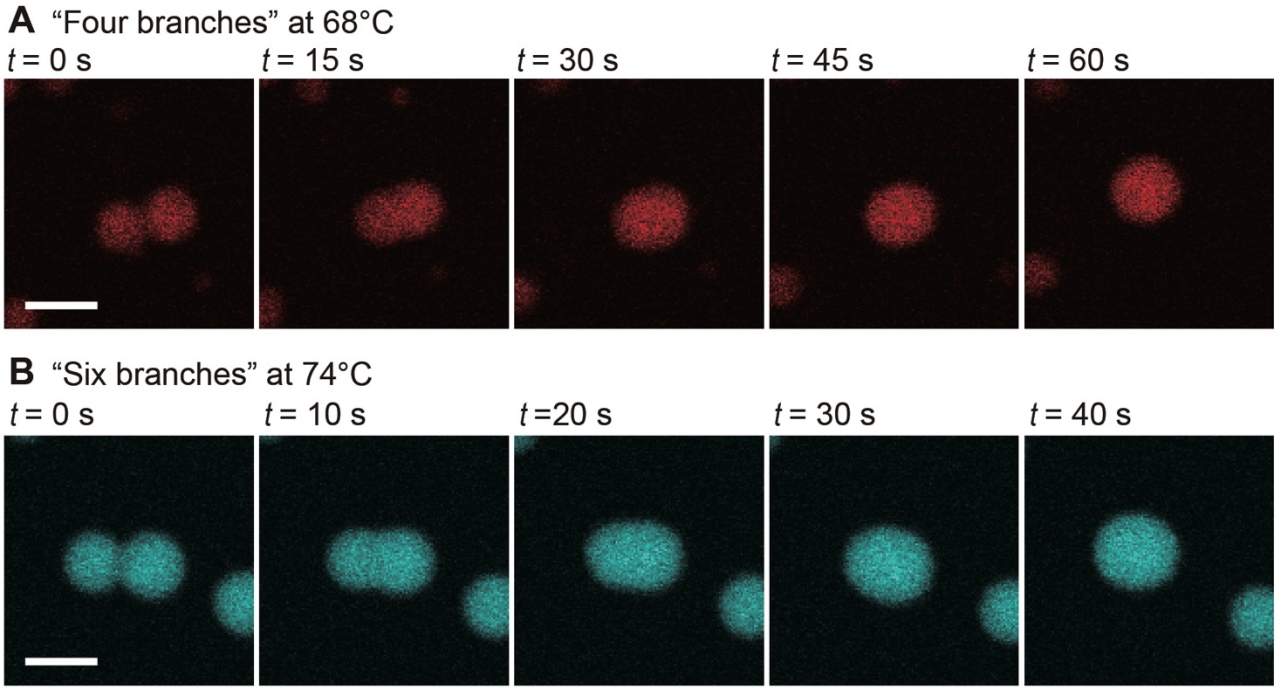

Fig. S10. **Fusion behavior of DNA droplets composed of motifs having four (A) and six (B) branches with 8-nucleotide sticky ends.** Scale bars: 10 μm.

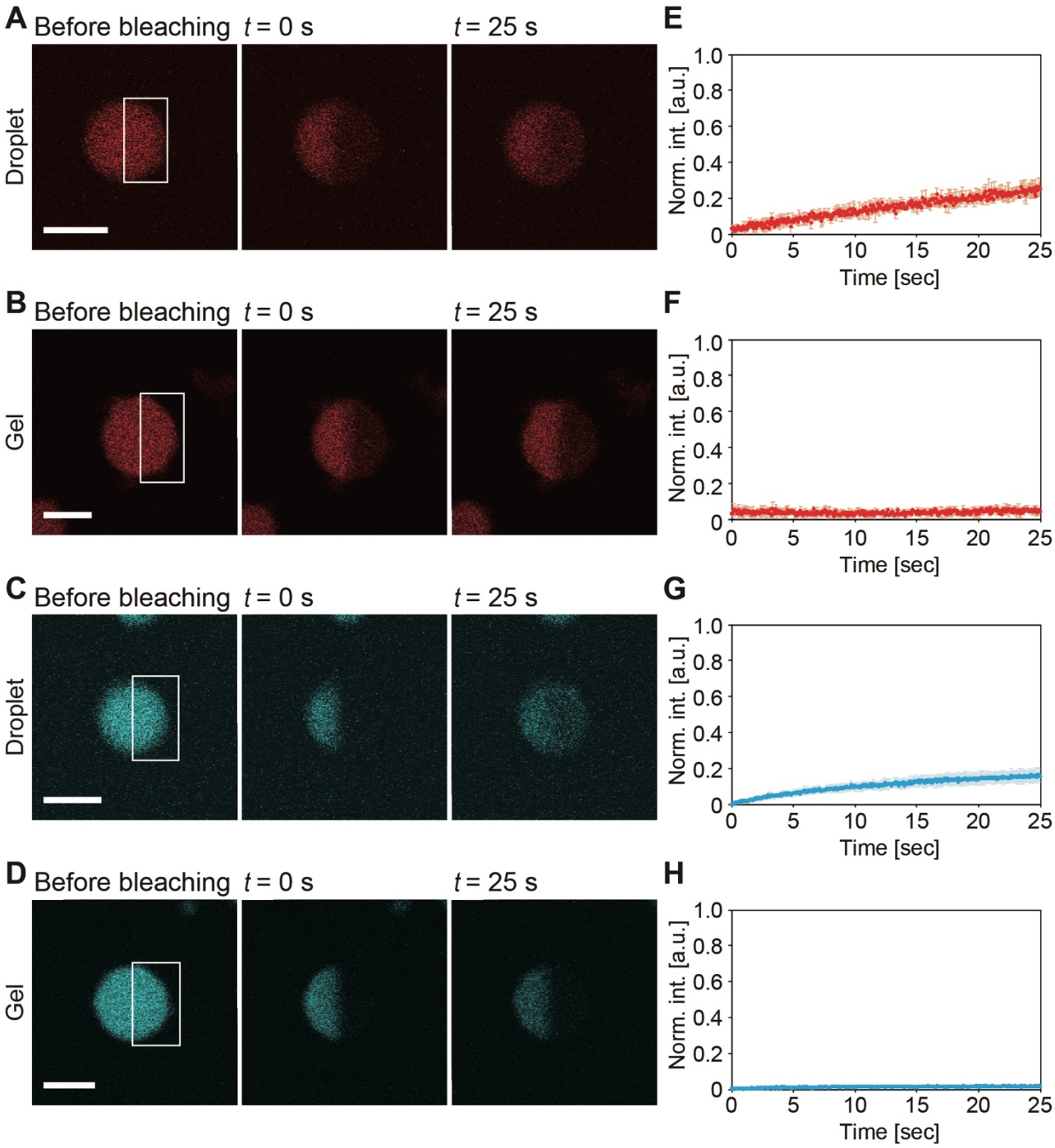

Fig. S11. **FRAP experiments for DNA droplets and hydrogels composed of motifs with four or six branches with 8-nucleotide sticky ends.** (**A**) and (**B**) Microscopy images of FRAP experiments for DNA droplets (**A**) and hydrogels (**B**) composed of motifs with four branches with 8-nucleotide sticky ends visualized at 68 and 52 °C, respectively. (**C**) and (**D**) Microscopy images in FRAP experiments for DNA droplets (**C**) and hydrogels (**D**) composed of motifs with six branches with 8-nucleotide sticky ends, visualized at 74 and 60 °C, respectively. The bleached region is indicated by a white box in each image. Scale bars: 10 μm. (**E**) to (**H**) Time series of fluorescence intensity corresponding to the images shown to the left of each graph. Bars show the mean ± standard deviation (S.D.). The number of measurements (n) = 3.

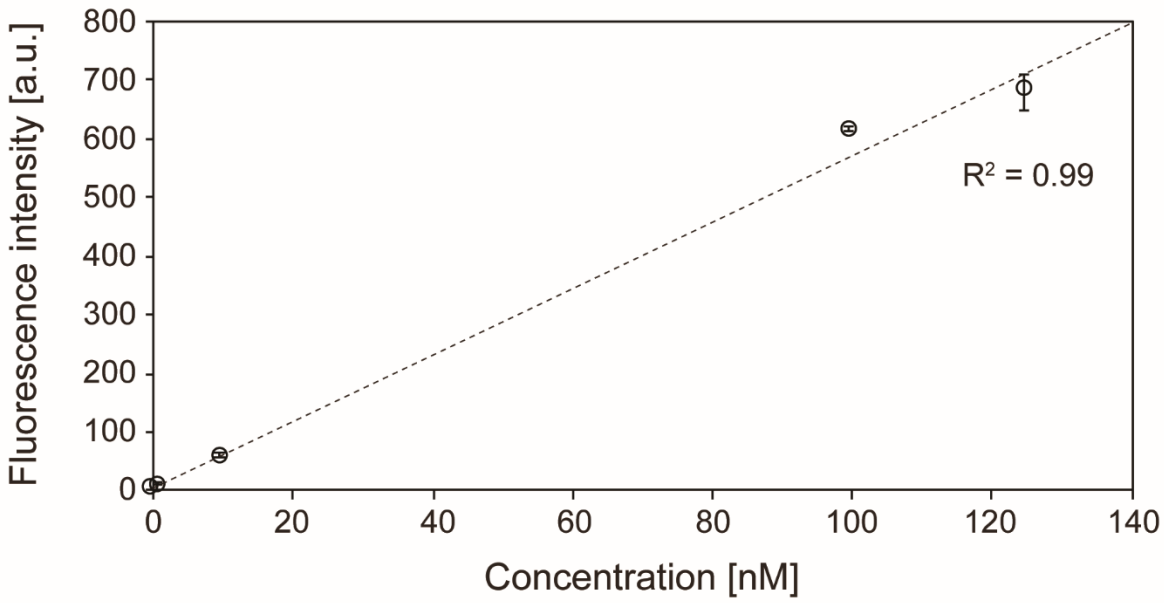

Fig. S12. **Calibration curve to estimate the concentration of Y-motifs in the droplet-like or gel states.** The dashed line through the center of the graph was obtained through linear fitting. R^2 is the deterministic coefficient. Error bars indicate standard deviation (mean ± S.D., n = 3).

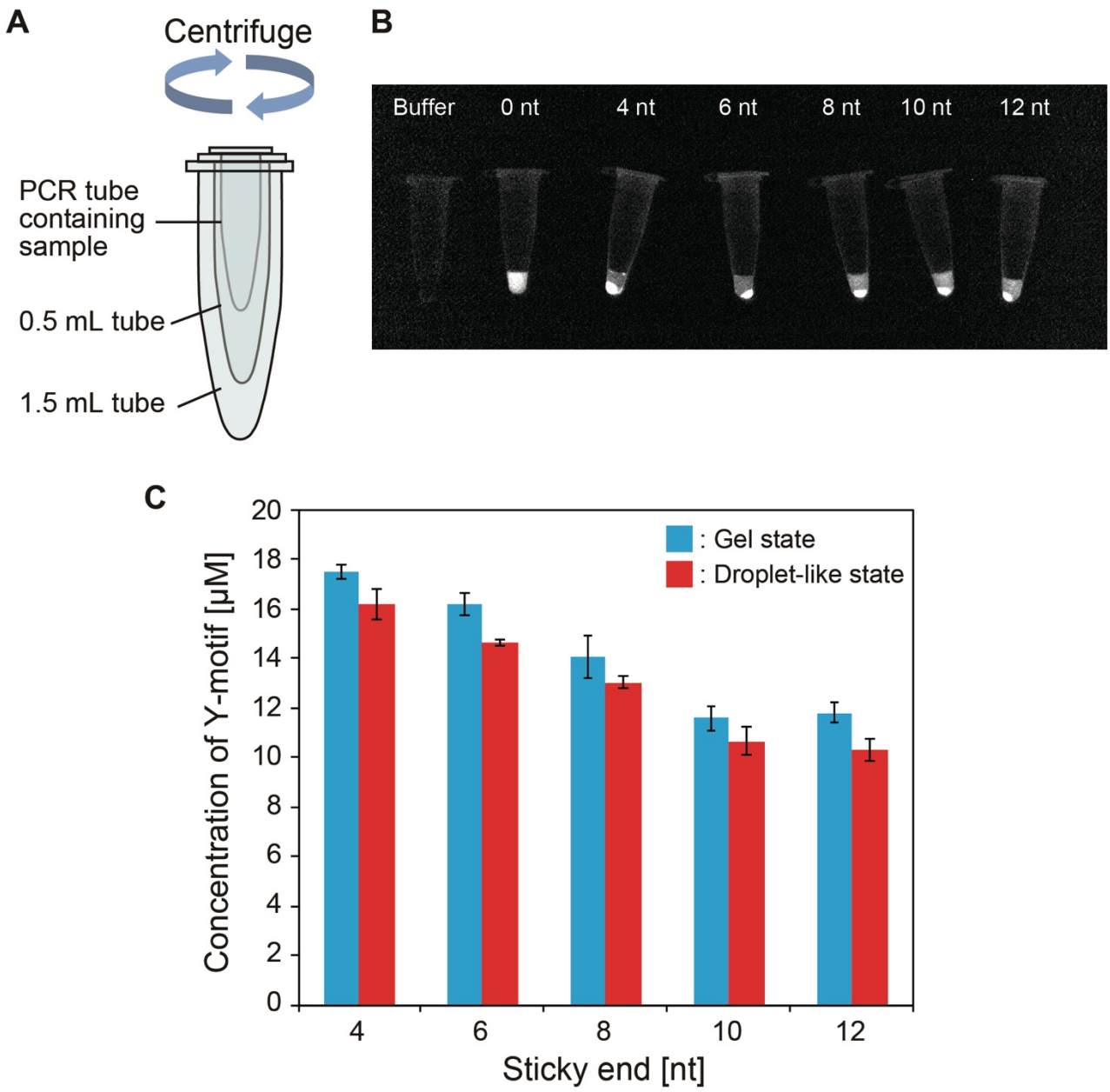

Fig. S13. Estimation of Y-motif concentration for each of the different nucleotide lengths of sticky ends. (**A**) Schematic illustration of the set-up. (**B**) Fluorescence photo images of the PCR tubes after centrifugation. (**C**) Estimates of the concentrations of Y-motifs with each length of sticky end in the droplet-like and gel states. Error bars indicate standard deviation (mean ± S.D., $n = 3$).

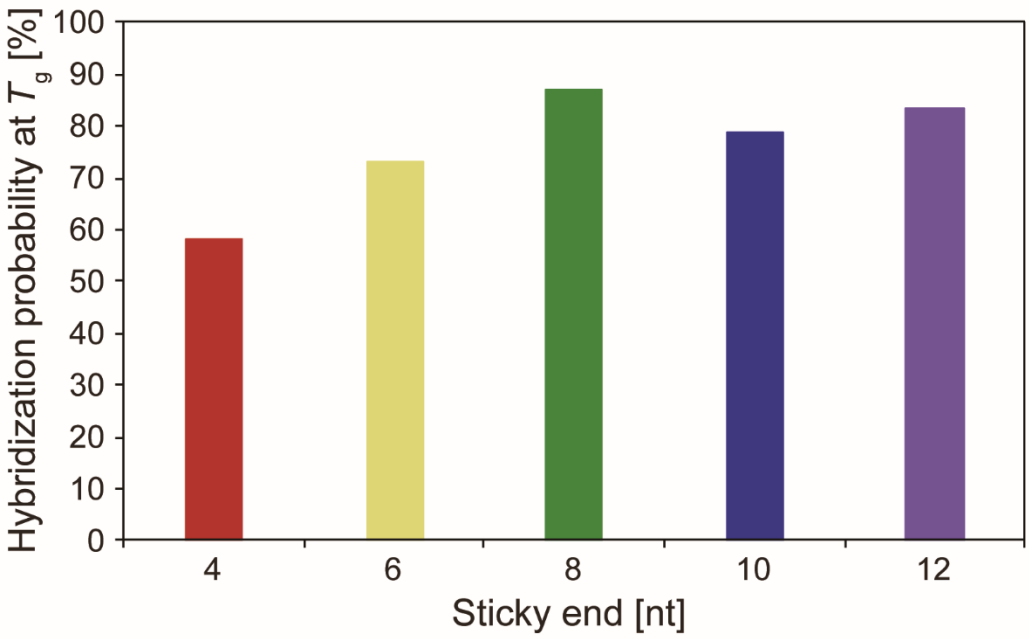

Fig. S14. Hybridization probability at T_g (the state-change temperature between the droplet-like and gel states) under the experimentally estimated concentrations of sticky ends. These values were obtained from numerical simulations using NUPACK software.

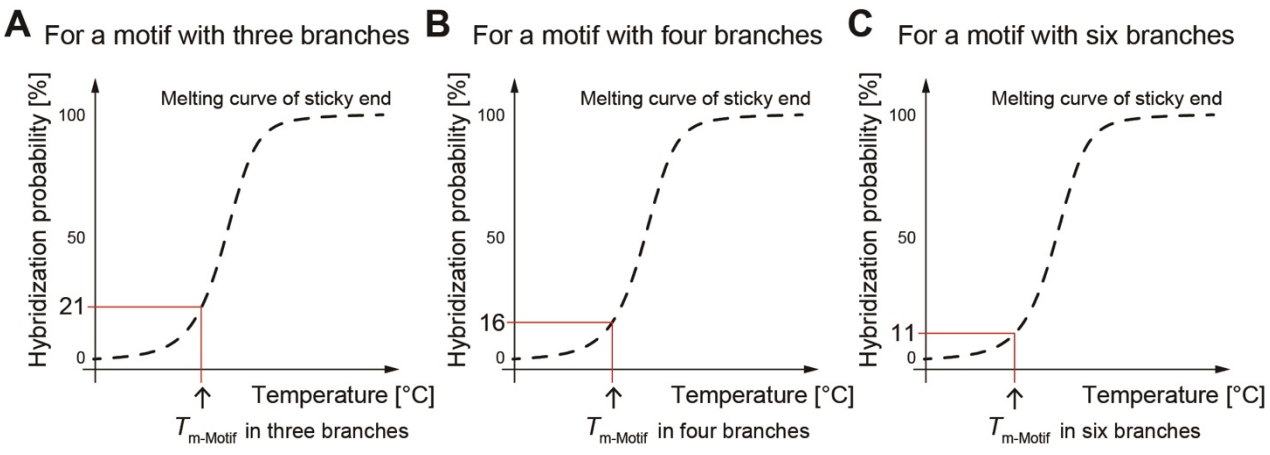

Fig. S15. **Definition of $T_{m\text{-}Motif}$, which represents the temperature at which at least one of the multiple sticky ends (SEs) can hybridize at a 50 % ratio.** To satisfy this, the hybridization probabilities of SEs in a motif with three, four, and six branches were 21, 16, 11 %, respectively.

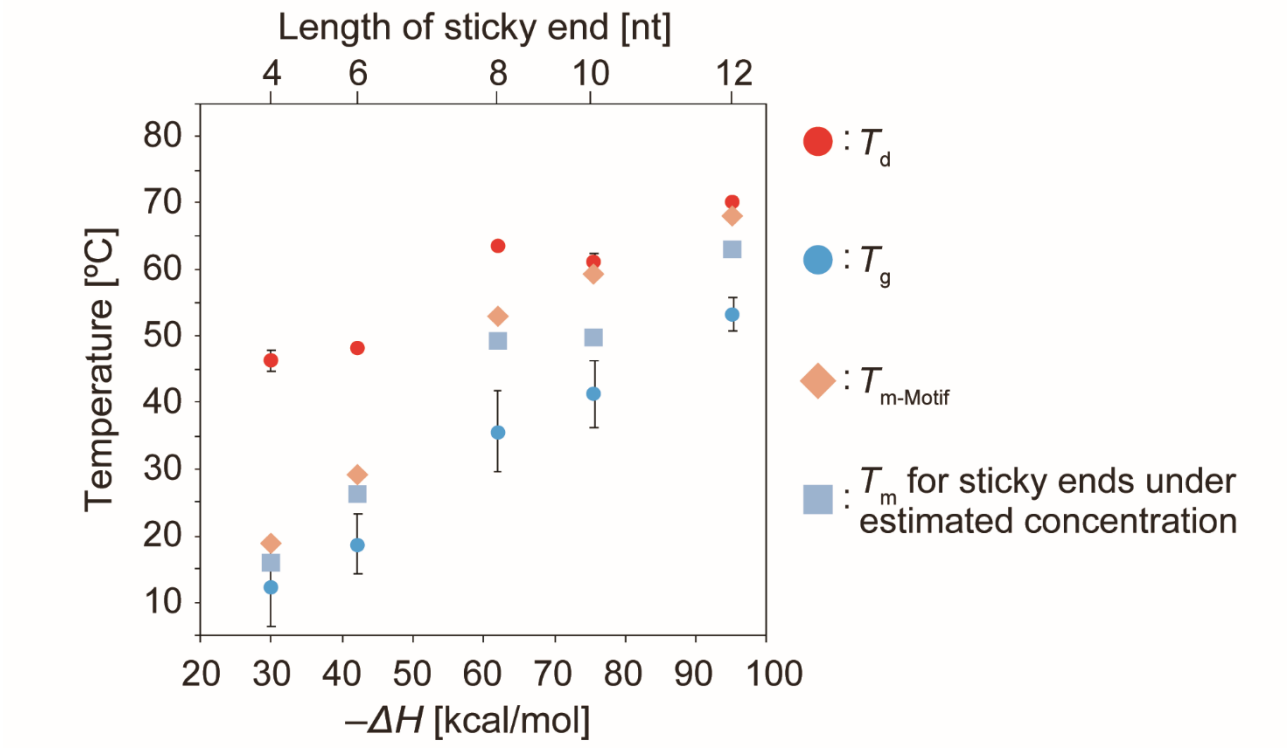

Fig. S16. Comparison of T_d (the state-change temperature between the dispersed and droplet-like states), T_g (the state-change temperature between the droplet-like and gel states), $T_{m\text{-}Motif}$ (the T_m for the motifs at which half of the motifs in a solution are connected), and T_m for the sticky ends with the experimentally estimated concentrations in the Y-motif with each length of sticky end. Error bars indicate standard deviation (mean ± S.D., n = 3).

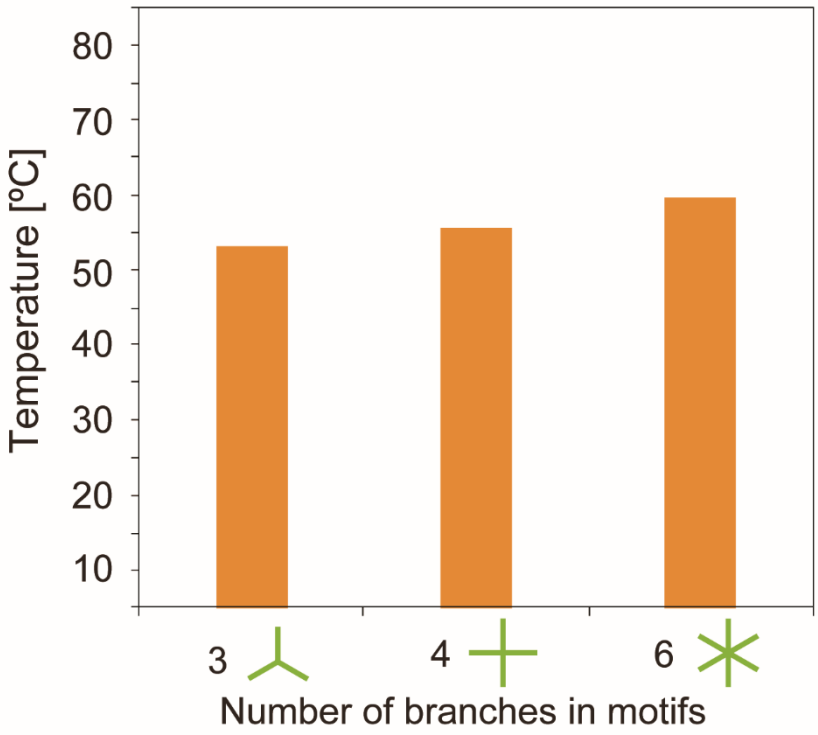

Fig. S17. $T_{m\text{-}Motif}$ **(the** T_m **for the motifs at which half of the motifs in a solution are connected) for DNA droplets with three, four, and six 8-nucleotide sticky ends.**

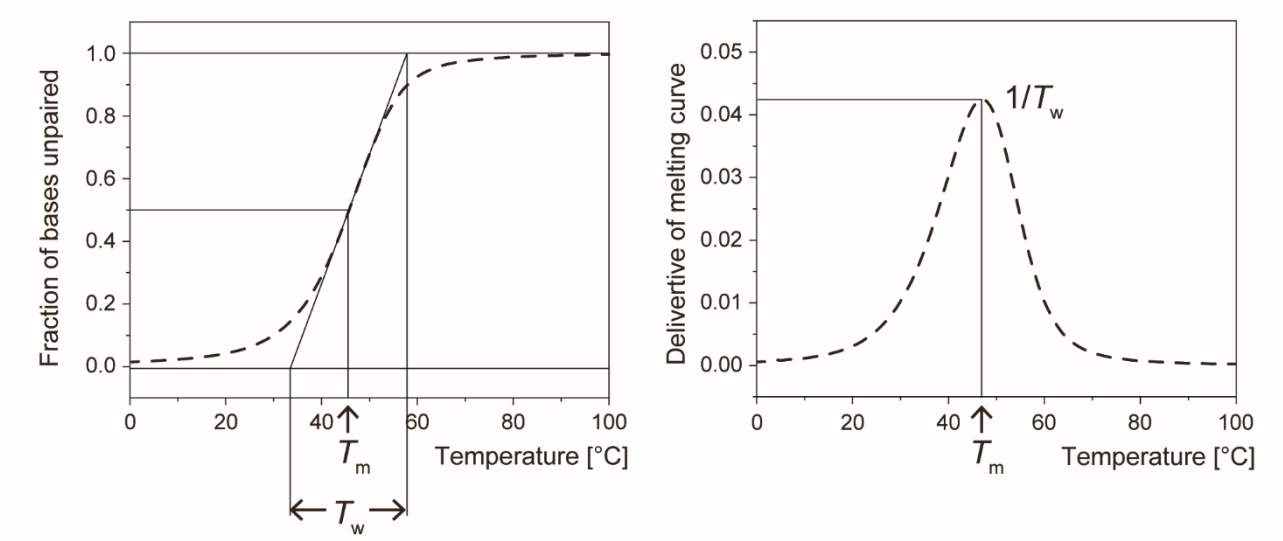

Fig. S18. **Definition of the width of the melting range (T_w).** T_w was determined as the distance between intersections with horizontal lines 'Fraction of bases unpaired' = 0 and 1 of the tangent in a melting curve at the T_m.

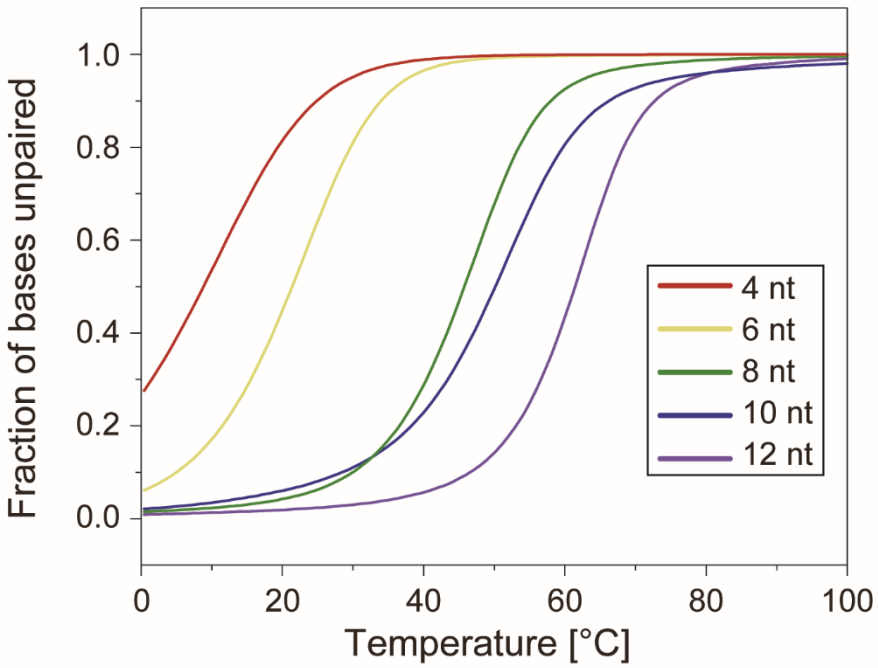

Fig. S19. Melting curves for sticky ends that are 4, 6, 8, 10, and 12 nucleotides in length obtained through numerical simulation using NUPACK software.

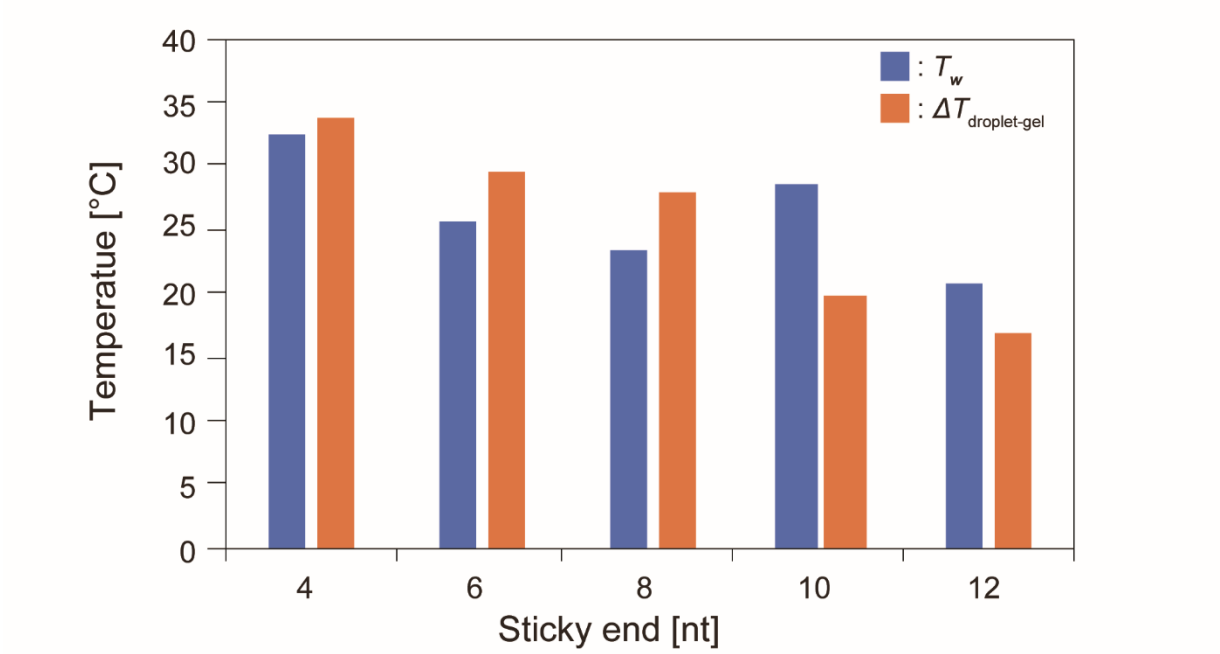

Fig. S20. Temperature differences between the T_d (the state-change temperature between the dispersed and droplet-like states), T_g (the state-change temperature between the droplet-like and gel states) ($\Delta T_{droplet\text{-}gel}$), and T_w (the width of the melting range) for the different nucleotide lengths of the sticky ends examined.

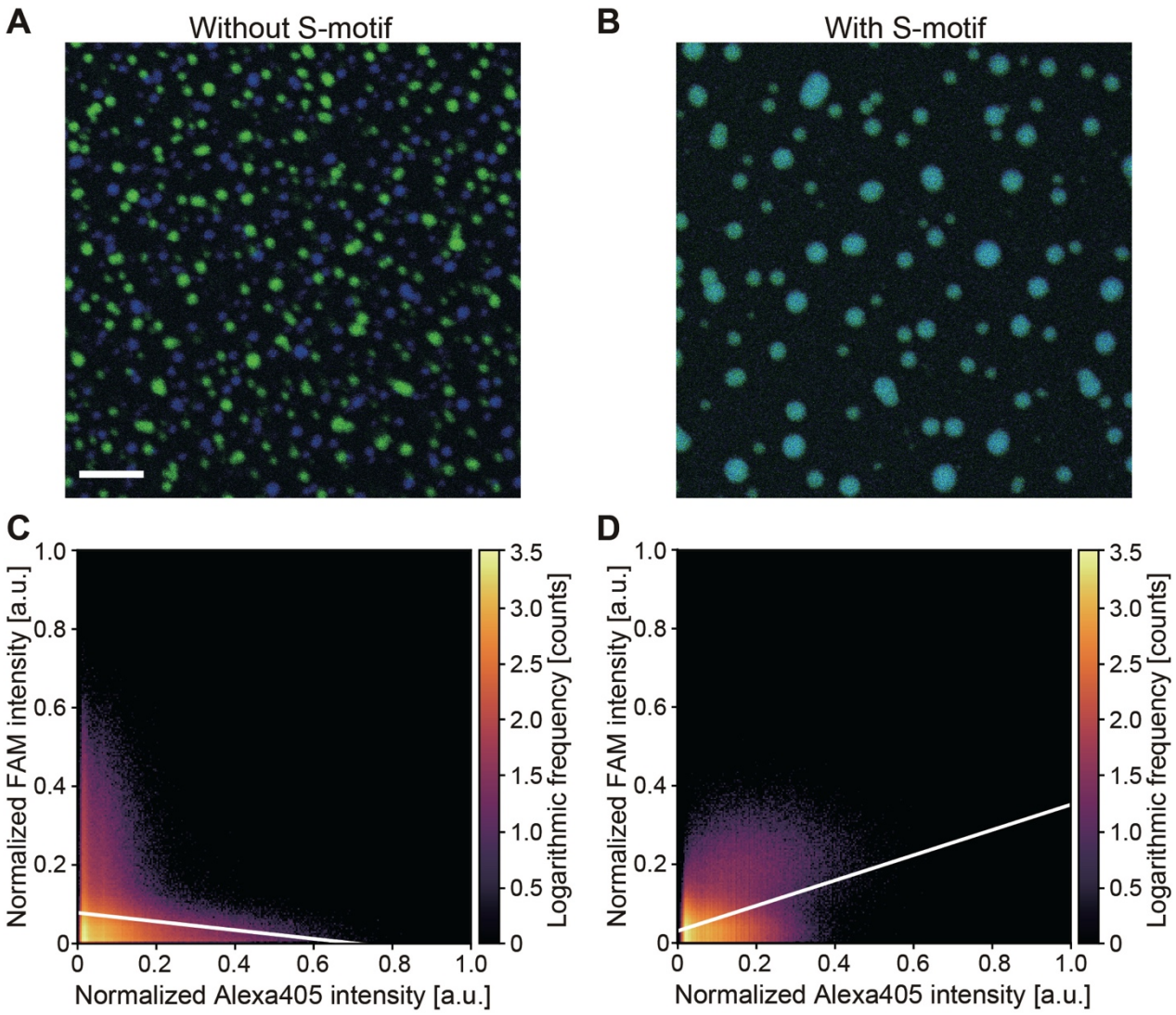

Fig. S21. **Colocalization analysis of FAM-labeled Y-motifs and Alexa405-labeled ^{orth}Y-motifs.** (**A**) and (**B**), Microscopy images of Y- and ^{orth}Y-motifs in droplet-like state without (**A**) and with S-motifs (**B**). Blue and green channels indicate ^{orth}Y- (Alexa405) and Y-motifs (FAM), respectively. Scale bar: 30 μm. (**C**) and (**D**), Two-dimensional histograms of the normalized intensity of FAM and Alexa405 without (**C**) and with S-motifs (**D**). White lines represent the linear regression line. In the graph without S-motifs, the slope of the line was negative, indicating a negative correlation between Y- and ^{orth}Y-motifs (C). In the graph with S-motifs, the slope of the line was positive, indicating a positive correlation (D).

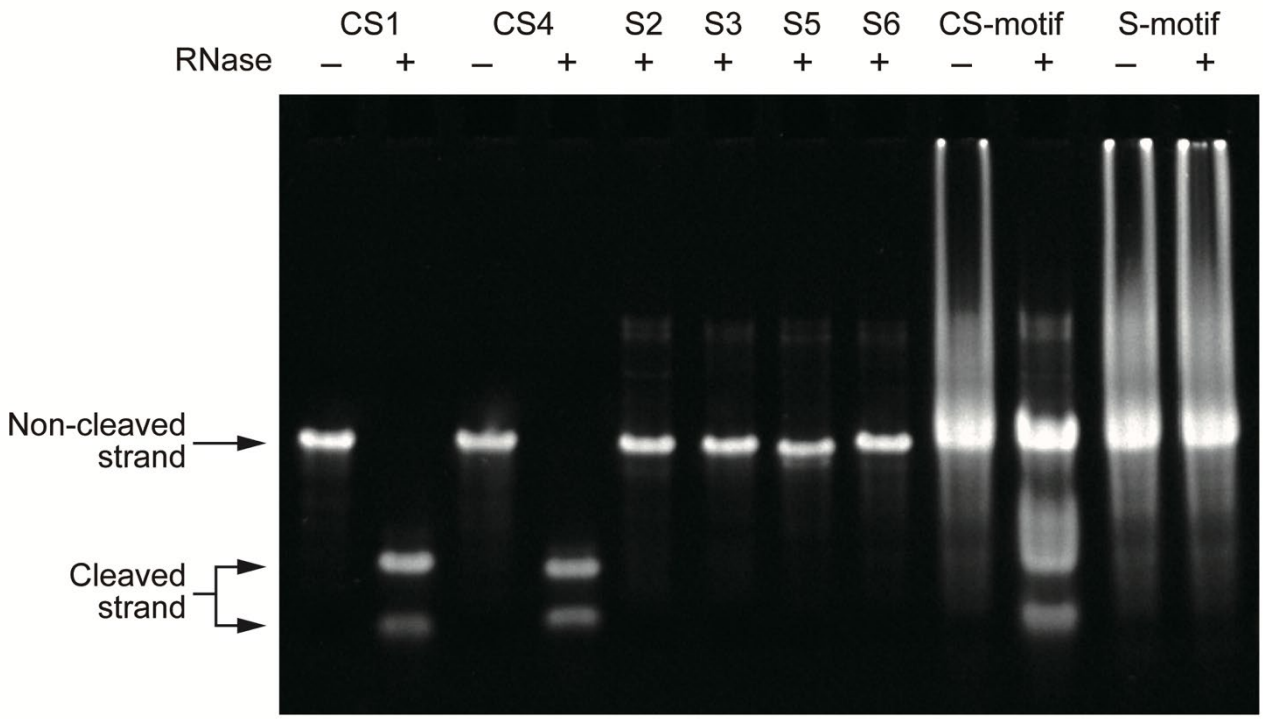

Fig. S22. **Denaturing gel electrophoresis of DNA–RNA chimera strands.** DNA–RNA chimera strands (CS1 and CS4) were successfully cleaved with RNase A, whereas the chimera strands without RNase A and the DNA strands (S2–S5) with and without RNase were not cleaved. Similarly, the chimera strands in the CS-motifs with RNase were cleaved, whereas the cleavage was not confirmed in the CS-motif without RNase A and in the S-motif with or without RNase.

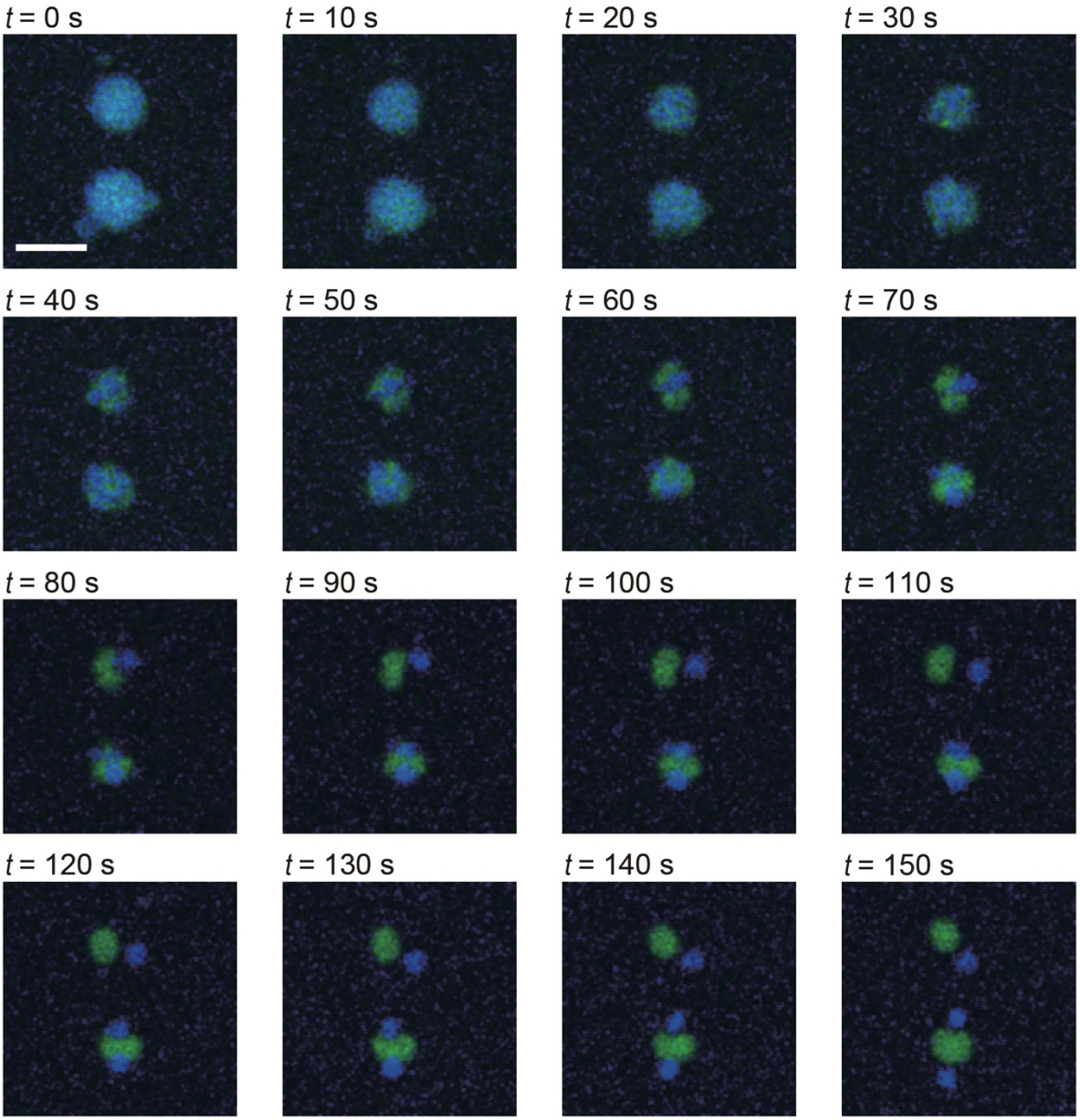

Fig. S23. **Detailed sequential microscopy images of the fission process of DNA droplets.** Blue and green channels indicate ^{orth}Y- and Y-motifs, respectively. Spinodal-like decomposition before the fission was observed during the fission process. We speculate that the driving force for the fission is electrical repulsion between ^{orth}Y- and Y-motifs. t = 0 s indicates 10 s after the addition of RNase. Scale bar: 20 μm.

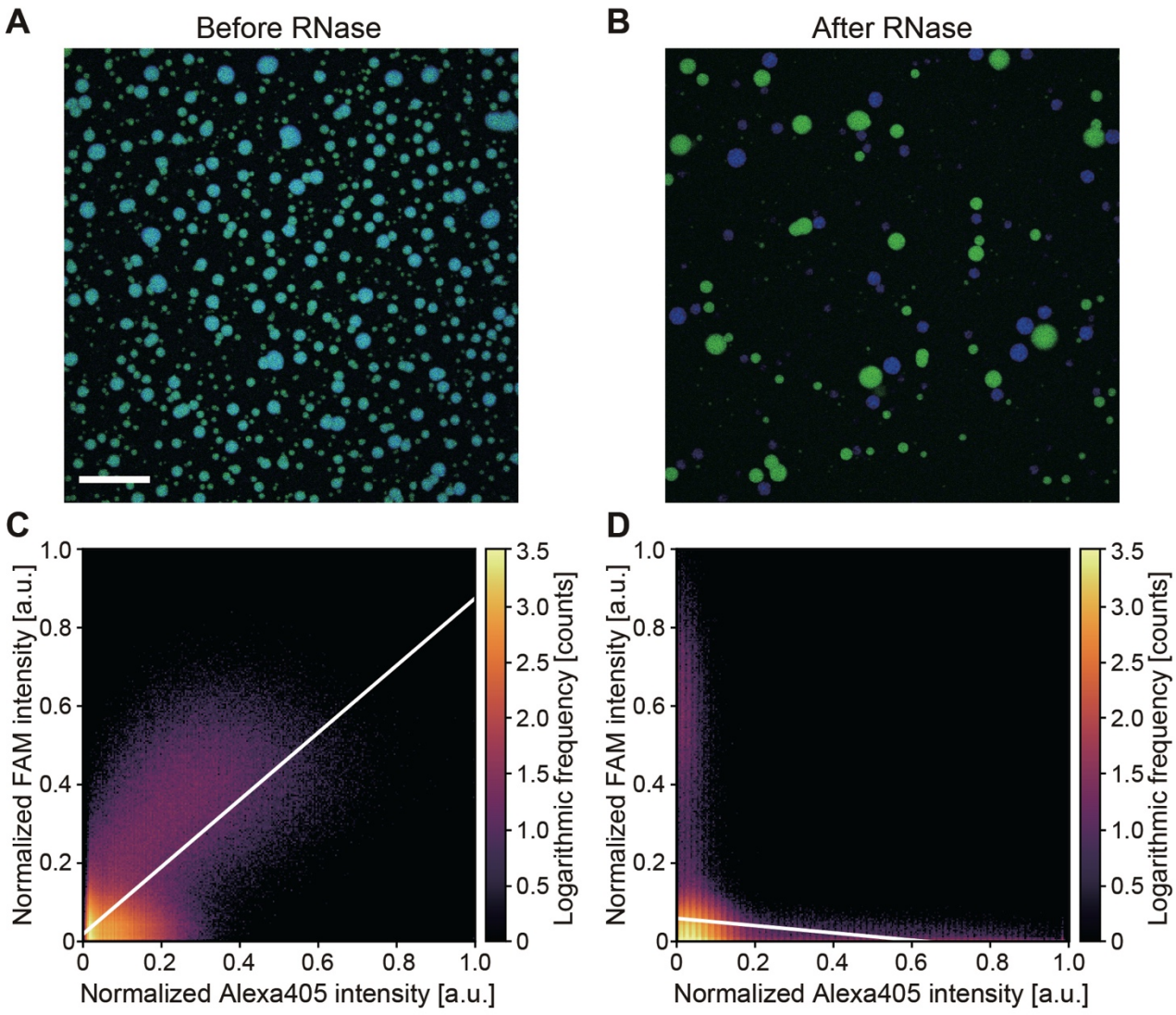

Fig. S24. **Colocalization analysis before and after addition of RNase A**. (**A**) and (**B**) Microscopic images of Y- and ^{orth}Y-motifs in the droplet-like state before (**A**) and after (**B**) addition of RNase A. Blue and green channels indicate ^{orth}Y- (Alexa405) and Y-motifs (FAM), respectively. Scale bar: 100 μm. (**C**) and (**D**) Two-dimensional histograms of the intensity of FAM and Alexa405 before (**C**) and after (**D**) addition of RNase A. White lines represent the linear regression line. Before the addition of RNase A, the slope of the line was positive, indicating a positive correlation between Y- and ^{orth}Y-motifs (C). After the addition, the slope of the line was negative, indicating a negative correlation (D).

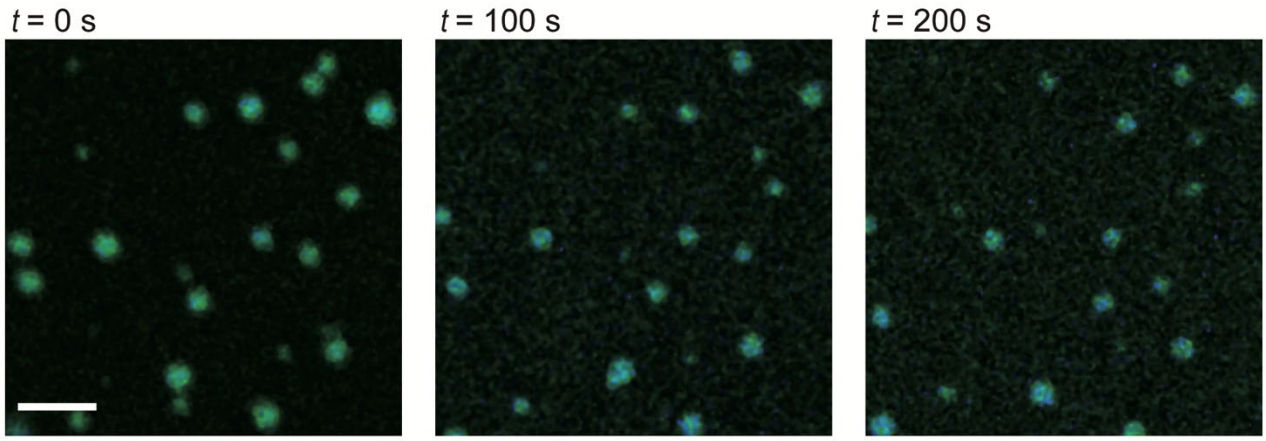

Fig. S25. **Droplet behavior after addition of buffer without RNase.** Blue and green channels indicate ^{orth}Y- (Alexa405) and Y-motifs (FAM), respectively. *t* = 0 s indicates 10 s after the addition of RNase. Scale bar: 20 μm.

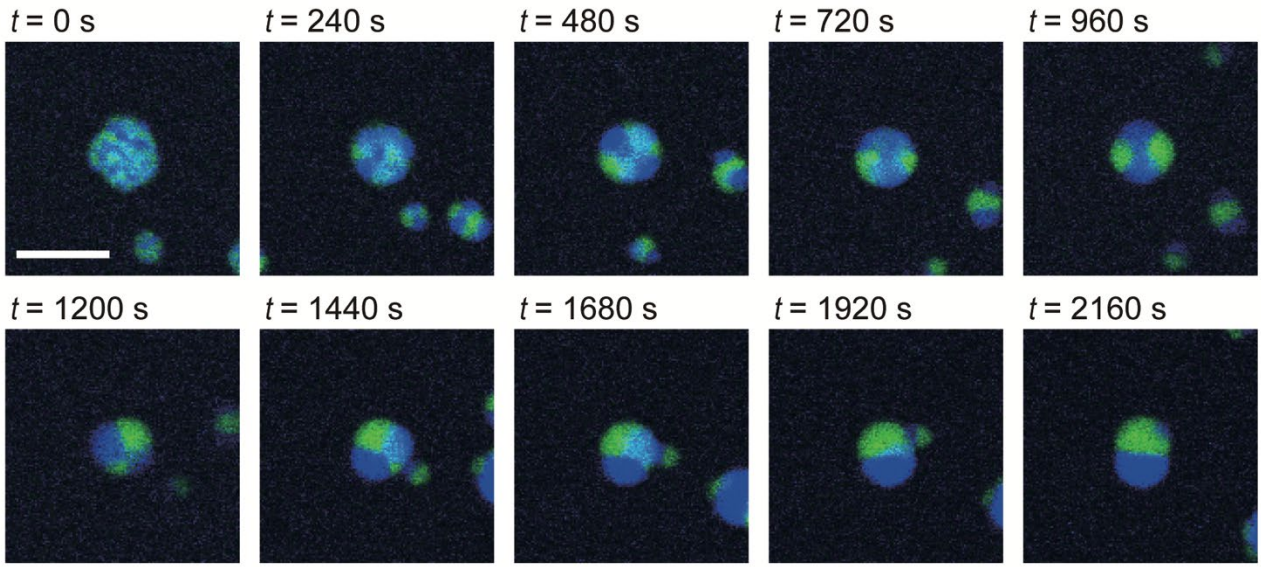

Fig. S26. **Sequential microscopy images of the formation process of the Janus shape.** Blue and green channels indicate ^{orth}Y- (Alexa405) and Y-motifs (FAM), respectively. Scale bar: 20 μm.

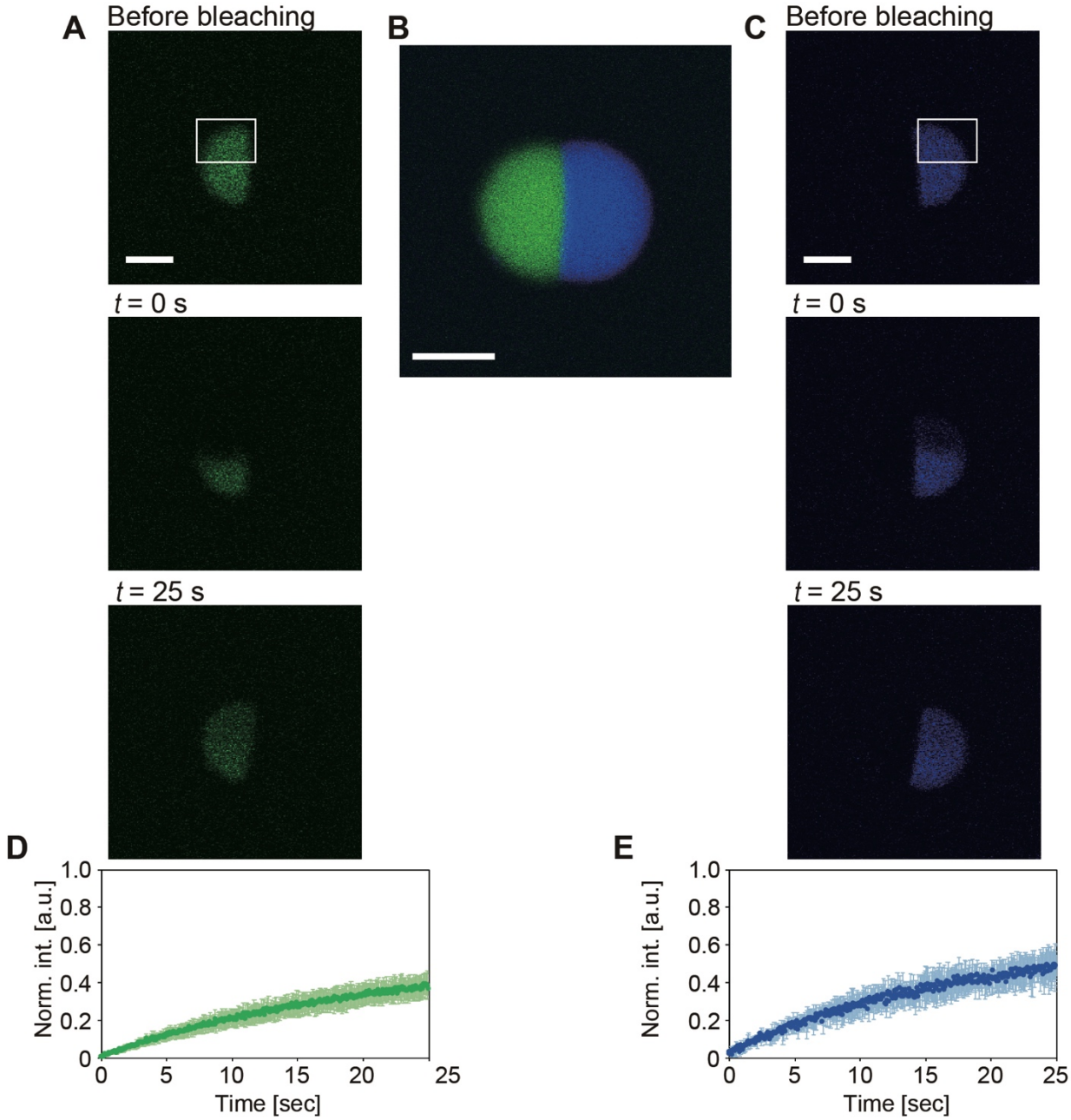

Fig. S27. **FRAP experiments to confirm the fluidity in both motifs in Janus droplets.** (**A**) and (**C**) Microscopy images from FRAP experiments for FAM-labeled Y-motifs (**A**) and Alexa405-labeled ^{orth}Y-motifs (**C**). The bleached region is indicated by a white box in each image. (**B**) Microscopy images of Janus droplets before photo-bleaching. Scale bars: 10 μm. (**D**) and (**E**) Time series of fluorescence intensity of FAM-labeled Y-motifs (**D**) and Alexa405-labeled ^{orth}Y-motifs (**E**). Error bars show standard deviation (n = 3).

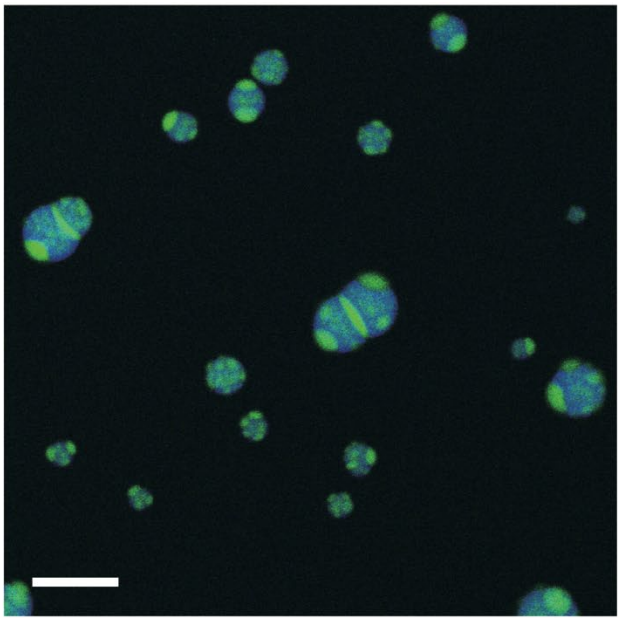

Fig. S28. **Patchy-like patterns in DNA droplets.** These were formed with 50 % DNA–RNA chimera strands in the CS-motifs after enzymatic reaction. Blue and green channels indicate ^{orth}Y- (Alexa405) and Y-motifs (FAM), respectively. The image was obtained 2 h after addition of RNase A. Scale bar: 30 μm.

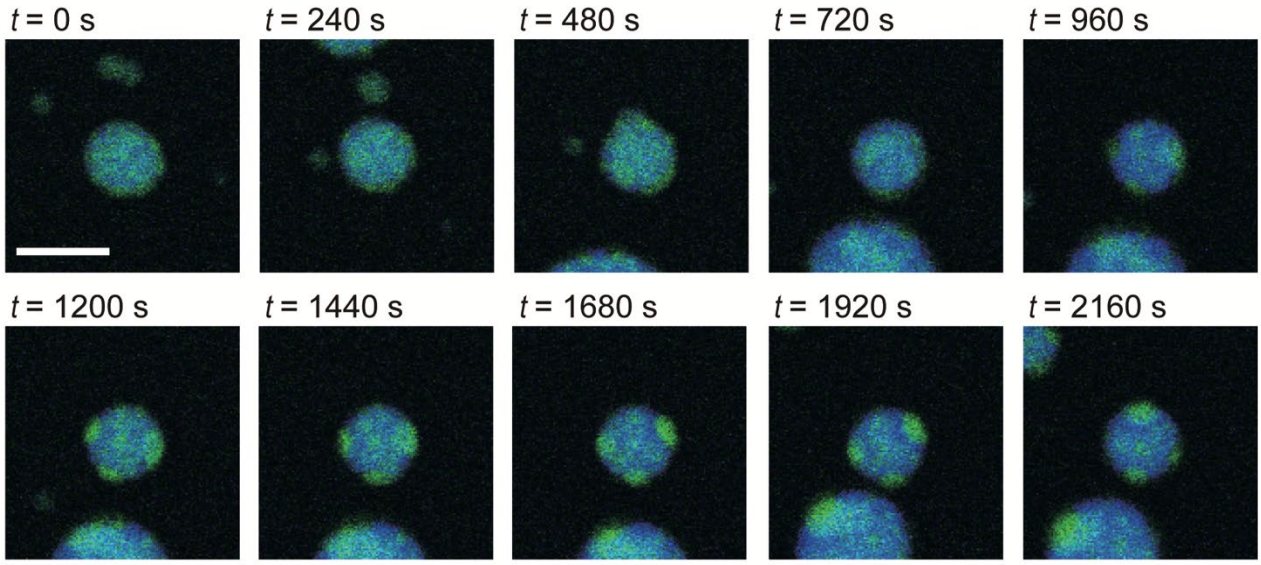

Fig. S29. **Sequential microscopy images of the formation process of patchy-like patterns.** Blue and green channels indicate ^{orth}Y- (Alexa405) and Y-motifs (FAM), respectively. Scale bar: 20 μm.

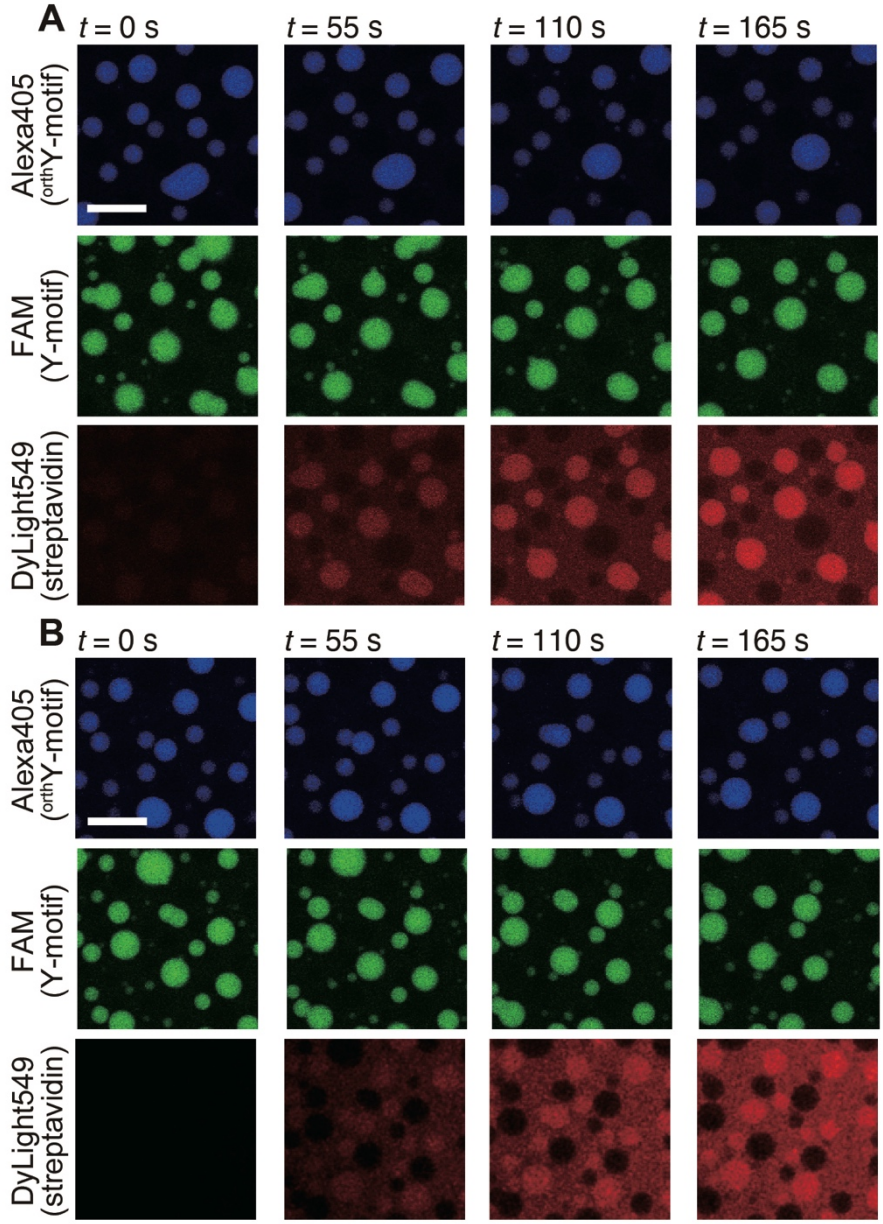

Fig. S30. **Sequential microscopy images of the accumulation process of DNA-modified streptavidin in DNA droplets composed of Y- (A) and ^{orth}Y-motifs (B).** Scale bars: 50 μm.

Captions for Supplementary Movies

Movie S1. Fusion of DNA droplets composed of Y-motifs with 8-nucleotide sticky ends. This movie was obtained at 63 °C. Scale bar: 30 μm.

Movie S2. Selective and exclusive fusion of DNA droplets composed of Y- or ^{orth}Y-motifs with 8-nucleotide sticky ends. Sequences of DNAs for the two motifs were not complementary. Blue and green channels indicate ^{orth}Y-(Alexa405) and Y-motifs (FAM), respectively. This movie was obtained at 64 °C. Scale bar: 30 μm.

Movie S3. Fission of DNA droplets composed of Y-, ^{orth}Y-, and chimerized-six-junction motifs with 8-nucleotide sticky ends. Blue and green channels indicate ^{orth}Y-(Alexa405) and Y-motifs (FAM), respectively. This movie was obtained at 65 °C. Filming began 10 s after addition of RNase A. Scale bar: 20 μm.